Table 4 Summary of adverse events and laboratory abnormalities during the 24-week blinded treatment phase

	ETV 0.01 mg ($n = 35$)	ETV 0.1 mg ($n = 34$)	ETV 0.5 mg ($n = 34$)	LVD 100 mg ($n = 34$)
Any adverse events	34 (97)	33 (97)	31 (91)	34 (100)
Most frequent clinical adverse events,[a] *n* (%)				
Nasopharyngitis	9 (25.7)	10 (29.4)	11 (32.4)	10 (29.4)
Headache	6 (17.1)	7 (20.6)	2 (5.9)	7 (20.6)
Diarrhea	1 (2.9)	1 (2.9)	4 (11.8)	4 (11.8)
Grade 3/4 clinical adverse events, *n* (%)	0	0	1 (2.9)	1 (2.9)
Grade 3/4 laboratory adverse events, *n* (%)	2 (5.7)	4 (11.8)	2 (5.9)	4 (11.8)
Any serious adverse events, *n* (%)	0	1 (2.9)	2 (5.9)	1 (2.9)
Discontinuations due to adverse events,[b] *n* (%)	0	0	1 (2.9)	1 (2.9)
ALT flares,[c] *n* (%)	0	1 (2.9)	1 (2.9)	2 (5.9)
Death, *n* (%)	0	0	0	0

[a] Occurring in at least 10% of patients

[b] One patient treated with ETV 0.5 mg discontinued the study drug due to hepatic cirrhosis. One patient treated with lamivudine discontinued due to increased ALT

[c] ALT flare defined ALT >2 × baseline and 10 × ULN

ETV entecavir

LVD lamivudine

diarrhea (Table 4). Grade 3/4 clinical adverse events occurred in one patient in the entecavir 0.5 mg group (colon carcinoma) and one patient in the lamivudine group (anal ulcer); neither of these events was considered to be related to the study drug. Serious adverse events were limited to the above-mentioned case of colon carcinoma, serum ALT elevation (entecavir 0.1 mg group [$n = 1$], entecavir 0.5 mg group [$n = 1$]), and serum aspartate aminotransferase (AST)/ALT elevation (lamivudine 100 mg group [$n = 1$]), but these were not considered to be causally related to the study drug and did not necessitate treatment discontinuation. Transient ALT flares (serum ALT >2 × baseline level and >10 × ULN) occurred in four patients (entecavir 0.1 mg group [$n = 1$], entecavir 0.5 mg group [$n = 1$], and lamivudine 100 mg group [$n = 2$]) and were associated with HBV DNA level decreases of 2 $\log_{10}$ copies/ml or more. None of the ALT flares were associated with hepatic decompensation and serum ALT and AST levels recovered to less than 1.25 × baseline level on continuation of the study treatment.

Discussion

The global ETV-005 study reported that entecavir was superior to lamivudine at reducing viral load in nucleoside-naive patients with CHB infection [15]. We conducted the present study, using an identical design to the ETV-005 study, to determine whether the findings from this earlier study are applicable to Japanese patients. In keeping with the previous findings, our results indicate that entecavir produces a dose-related reduction in serum HBV DNA level ($0.01 < 0.1 \leq 0.5$ mg) in nucleoside-naive Japanese patients with CHB; the log dose–response curves for the reduction in serum HBV DNA level with entecavir in the two studies were similar, with estimated regression curve slopes of –1.24 (Japanese study) and –1.32 (global study). In addition, both studies demonstrated the noninferiority of the entecavir 0.1 mg group compared with the lamivudine 100 mg group and the superiority of the entecavir 0.5 mg group compared with the lamivudine 100 mg group. The demonstration of a dose–response relationship for entecavir and the superiority of the entecavir 0.5 mg dose over lamivudine confirm that the antiviral activity of entecavir in Japanese patients is similar to that observed in study ETV-005. In a previous study, Ono et al. [14] demonstrated that the in vitro potency of entecavir was up to 2,200 times greater than that of lamivudine. The results presented here substantiate these earlier in vitro data and confirm the greater potency of entecavir over lamivudine in patients with CHB.

Serum ALT normalization rates with entecavir 0.5 mg and lamivudine 100 mg (~80%) were higher in the present study than those reported in the ETV-005 study (entecavir 0.5 mg, 69.0%; lamivudine 100 mg, 59.1%) [15]. In keeping with previous findings [20, 21], the incidence of entecavir-associated serum ALT flares in Japanese patients was low. The serum ALT flares occurred against a background of 2 $\log_{10}$ copies/ml or more reductions in serum

HBV DNA level, and serum ALT levels subsequently normalized without discontinuation of entecavir. Therefore, the serum ALT flare noted here may indicate recovery of the host's immune response arising from the reduction in HBV viral titer [22, 23]. ALT flares have been reported after the discontinuation of entecavir therapy [15, 16], thus necessitating long-term follow-up to identify possible posttreatment viral rebound.

In conclusion, the results of this dose-ranging study demonstrate a clear dose–response relationship for entecavir in terms of mean HBV DNA level reduction at week 22. Entecavir 0.5 mg was significantly more effective than lamivudine 100 mg in reducing HBV DNA levels in nucleoside-naive Japanese adult patients with CHB. At this dose level, entecavir treatment resulted in serum HBV DNA levels of less than 400 copies/ml in 100% of patients and normalization of serum ALT levels in 80% of patients after 22 weeks. Moreover, entecavir 0.5 mg once daily was well tolerated and showed a comparable safety profile to lamivudine.

References

1. Maddrey WC. Hepatitis B: an important public health issue. J Med Virol 2000;61:362–366. doi:10.1002/1096-9071(200007)61:3<362::AID-JMV14>3.0.CO;2-I
2. Kao JH, Chen DS. The natural history of hepatitis B virus infection. In Lai CL, Locarnini S, editors. Hepatitis B Virus. London: International Medical Press; 2002. 161–172
3. Lok AS, McMahon BJ. American Association for the Study of Liver Diseases (AASLD) practice guidelines. Chronic Hepatitis B. Hepatology 2007;45:507–539. doi:10.1002/hep.21513
4. Rivkin A. A review of entecavir in the treatment of chronic hepatitis B infection. Curr Med Res Opin 2005;21:1845–1856. doi:10.1185/030079905X65268
5. Wong DKH, Cheung AM, O'Rourke K, Naylor CD, Detsky AS, Heathcote J. Effect of alpha-interferon treatment in patients with hepatitis B e antigen-positive chronic hepatitis B. A meta-analysis. Ann Intern Med 1993;119:312–323
6. Allen MI, Deslauriers M, Andrews CW, Tipples GA, Walters KA, Tyrrell DL, et al. Identification and characterization of mutations in hepatitis B virus resistant to lamivudine. Lamivudine Clinical Investigation Group. Hepatology 1998;27:1670–1677. doi:10.1002/hep.510270628
7. Chang TT, Lai CL, Chien RN, Guan R, Lim SG, Lee CM, et al. Four years of lamivudine treatment in Chinese patients with chronic hepatitis B. J Gastroenterol Hepatol 2004;19(11):1276–1282. doi:10.1111/j.1440-1746.2004.03428.x
8. Liaw YF, Sung JJ, Chow WC, Farrell G, Lee CZ, Yuen H, et al. Lamivudine for patients with chronic hepatitis B and advanced liver disease. N Engl J Med 2004;351(15):1521–1531. doi:10.1056/NEJMoa033364
9. Omata M. Treatment of chronic hepatitis B infection. N Engl J Med 1998;339:114. doi:10.1056/NEJM199807093390209
10. Liaw YF, Leung N, Kao JH, Piratvisuth T, Gane E, Han KH, et al. Asian-Pacific consensus statement on the management of chronic hepatitis B: a 2008 update. Hepatol Int 2008;2:263–283. doi:10.1007/s12072-008-9080-3
11. Genovesi EV, Lamb L, Medina I, Taylor D, Seifer M, Innaimo S, et al. Efficacy of the carbocyclic 2′-deoxyguanosine nucleoside BMS-200475 in the woodchuck model of hepatitis B virus infection. Antimicrob Agents Chemother 1998;42:3209–3217
12. Marion PL, Salazar FH, Winters MA, Colonno RJ. Potent efficacy of entecavir (BMS-200475) in a duck model of hepatitis B virus replication. Antimicrob Agents Chemother 2002;46:82–88. doi:10.1128/AAC.46.1.82-88.2002
13. Colonno RJ, Rose R, Baldick CJ, Levine S, Pokornowski K, Yu CF, et al. Entecavir resistance is rare in nucleoside naïve patients with hepatitis B. Hepatology 2006;44:1656–1665. doi:10.1002/hep.21422
14. Ono SK, Kato N, Shiratori Y, Kato J, Goto T, Schinazi RF, et al. The polymerase L528M mutation cooperates with nucleotide binding-site mutations, increasing hepatitis B virus replication and drug resistance. J Clin Invest 2001;107:449–455. doi:10.1172/JCI11100
15. Lai CL, Rosmawati M, Lao J, Van Vlierberghe H, Anderson FH, Thomas N, et al. Entecavir is superior to lamivudine in reducing hepatitis B virus DNA in patients with chronic hepatitis B infection. Gastroenterology 2002;123:1831–1838. doi:10.1053/gast.2002.37058
16. Chang TT, Gish RG, Hadziyannis SJ, Cianciara J, Rizzetto M, Schiff ER, et al. A dose-ranging study of the efficacy and tolerability of entecavir in lamivudine-refractory chronic hepatitis B patients. Gastroenterology 2005;129:1198–1209. doi:10.1053/j.gastro.2005.06.055
17. Ling R, Mutimer D, Ahmed M, Boxall EH, Elias E, Dusheiko GM, et al. Selection of mutations in the hepatitis B virus polymerase during therapy of transplant recipients with lamivudine. Hepatology 1996;24:711–713. doi:10.1002/hep.510240339
18. Tipples GA, Ma MM, Fischer KP, Bain VG, Kneteman NM, Tyrrell DLJ. Mutation in HBV RNA-dependent DNA polymerase confers resistance to lamivudine in vivo. Hepatology 1996;24:714–717
19. Tenney DJ, Levine SM, Rose RE, Walsh AW, Weinheimer SP, Discotto L, et al. Clinical emergence of entecavir-resistant hepatitis B virus requires additional substitutions in virus already resistant to lamivudine. Antimicrob Agents Chemother 2004;48:3498–3507. doi:10.1128/AAC.48.9.3498-3507.2004
20. Chang TT, Gish R, de Man R, Gadano A, Sollano J, Chao YC, et al. A comparison of entecavir and lamivudine for HBeAg-positive chronic hepatitis B. N Engl J Med 2006;354:1074–1076. doi:10.1056/NEJMoa051285
21. Sherman M, Yurdaydin C, Sollano J, Silva M, Liaw Y-F, Cianciara J, et al. Entecavir is superior to continued lamivudine for the treatment of lamivudine-refractory. HBeAg-positive chronic hepatitis B. Gastroenterology 2006;130:2039–2049
22. Boni C, Bertoletti A, Penna A, Cavalli A, Pilli M, Urbani S, et al. Lamivudine treatment can restore T cell responsiveness in chronic hepatitis B. J Clin Invest 1998;102:968–975. doi:10.1172/JCI3731
23. Nair S, Perrillo RP. Serum alanine aminotransferase flares during interferon treatment of chronic hepatitis B: is sustained clearance of HBV DNA dependent on levels of pretreatment viremia? Hepatology 2001;34:1021–1026. doi:10.1053/jhep.2001.28459

BMS9RJ3389

GENES, CHROMOSOMES & CANCER 48:109–120 (2009)

RESEARCH ARTICLES

ERK5 is a Target for Gene Amplification at 17p11 and Promotes Cell Growth in Hepatocellular Carcinoma by Regulating Mitotic Entry

Keika Zen,[1] Kohichiroh Yasui,[1]* Tomoaki Nakajima,[1] Yoh Zen,[2] Kan Zen,[3] Yasuyuki Gen,[1] Hironori Mitsuyoshi,[1] Masahito Minami,[1] Shoji Mitsufuji,[1] Shinji Tanaka,[4] Yoshito Itoh,[1] Yasuni Nakanuma,[2] Masafumi Taniwaki,[5] Shigeki Arii,[4] Takeshi Okanoue,[1] and Toshikazu Yoshikawa[1]

[1]Molecular Gastroenterology and Hepatology, Graduate School of Medical Science, Kyoto Prefectural University of Medicine, Kyoto, Japan
[2]Department of Human Pathology, Kanazawa University Graduate School of Medicine, Kanazawa, Japan
[3]Division of Cardiovascular Medicine, Omihachiman Community Medical Center, Omihachiman, Japan
[4]Department of Hepato-Biliary-Pancreatic Surgery, Tokyo Medical and Dental University, Tokyo, Japan
[5]Molecular Hematology and Oncology, Graduate School of Medical Science, Kyoto Prefectural University of Medicine, Kyoto, Japan

Using high-density oligonucleotide microarrays, we investigated DNA copy-number aberrations in cell lines derived from hepatocellular carcinomas (HCCs) and detected a novel amplification at 17p11. To identify the target of amplification at 17p11, we defined the extent of the amplicon and examined HCC cell lines for expression of all seven genes in the 750-kb commonly amplified region. Mitogen-activated protein kinase (MAPK) 7, which encodes extracellular-regulated protein kinase (ERK) 5, was overexpressed in cell lines in which the gene was amplified. An increase in *MAPK7* copy number was detected in 35 of 66 primary HCC tumors. Downregulation of *MAPK7* by small interfering RNA suppressed the growth of SNU449 cells, the HCC cell line with the greatest amplification and overexpression of *MAPK7*. ERK5, phosphorylated during the G2/M phases of the cell cycle, regulated entry into mitosis in SNU449 cells. In conclusion, our results suggest that *MAPK7* is likely the target of 17p11 amplification and that the ERK5 protein product of *MAPK7* promotes the growth of HCC cells by regulating mitotic entry.

INTRODUCTION

Hepatocellular carcinoma (HCC) is the fifth most common malignancy in the world and is estimated to cause approximately half a million deaths annually (El-Serag, 2002). Several risk factors for HCC have been reported, including infection with hepatitis B and C viruses, dietary intake of afratoxin, alcohol consumption, and diabetes.

The mitogen-activated protein kinase (MAPK) cascades transmit extracellular signals from cell surface receptors to specific intracellular targets and regulate a wide variety of cellular functions, including cell proliferation, differentiation, and the stress response (Nishimoto and Nishida, 2006). Extracellular stimuli induce sequential activation of MAPK kinase kinase, MAPK kinase, and MAPK. At least four MAPK subfamilies have been identified: extracellular-regulated protein kinase (ERK) 1 and 2, c-Jun-N-terminal kinases, p38, and ERK5 (also know as BMK1). ERK5, which was recently characterized, can be activated by a wide range of growth factors and cellular stresses, including serum, epithelial growth factor, oxidative stress, and hyperosmotic shock (Hayashi and Lee, 2004; Nishimoto and Nishida, 2006; Wang and Tournier, 2006). When stimulated, MAP/ERK kinase kinase 2 and 3 activate MAP/ERK kinase (MEK) 5, a specific kinase for ERK5. Subsequently, MEK5 phosphorylates ERK5, and the activated ERK5 promotes cell proliferation, differentiation, and survival (Hayashi and Lee, 2004; Garaude et al., 2006; Nishimoto and Nishida, 2006; Wang and Tournier, 2006). Some investigators have described the possible involvement of ERK5 in cancers (Esparis-Ogando et al., 2002; Weldon et al., 2002; Mulloy et al., 2003; Carvajal-Vergara et al., 2005; Linnerth et al., 2005).

Additional Supporting Information may be found in the online version of this article.

Supported by: Grants-in-Aid for Scientific Research from the Japan Society for the Program of Science, Grant number: 18390223.

*Correspondence to: Kohichiroh Yasui, Molecular Gastroenterology and Hepatology, Graduate School of Medical Science, Kyoto Prefectural University of Medicine, 465 Kajii-cho, Kamigyo-ku, Kyoto, 602-8566, Japan. E-mail: yasuik@koto.kpu-m.ac.jp

Received 24 May 2008; Accepted 11 September 2008

DOI 10.1002/gcc.20624

Published online 30 October 2008 in Wiley InterScience (www.interscience.wiley.com).

Accumulating evidence suggests that multiple sequential genetic alterations in a cell lineage at the nucleotide and chromosome levels underlie the carcinogenesis of solid tumors. Amplification of chromosomal DNA is one mechanism of activating genes whose overexpression contributes to the development and progression of cancer. Regions of chromosomal amplification in cancer cells frequently harbor oncogenes, such as *MYC* (Little et al., 1983) and *ERBB2* (Di Fiore et al., 1987). Using comparative genomic hybridization (CGH), we have detected novel regions of amplification in a variety of cancer types, including HCC, and we have identified a number of candidate oncogenes from amplicons (Yasui et al., 2001; Yasui et al., 2002; Yokoi et al., 2002; Okamoto et al., 2003; Yokoi et al., 2003). CGH was initially used for genome-wide detection of copy number changes occurring in cancers (Kallioniemi et al., 1992). However, its resolution is limited (5–10 Mb) because it detects segmental copy number changes on metaphase chromosomes.

The recent introduction of high-density oligonucleotide microarrays designed for typing of single nucleotide polymorphisms (SNPs) facilitates high-resolution mapping of chromosomal amplifications, deletions, and loss of heterozygosity (Mei et al., 2000; Bignell et al., 2004; Matsuzaki et al., 2004a,b; Wong et al., 2004; Zhao et al., 2004). The Affymetrix GeneChip Mapping 100K array set contains 116,204 SNP loci with a mean intermarker distance of 23.6 kb, and it enables detailed and genome-wide identification of DNA copy number changes (Matsuzaki et al., 2004a,b; Garraway et al., 2005; Zhao et al., 2005). The newer GeneChip Mapping 500K array set is composed of two arrays, each capable of genotyping an average 250,000 SNPs.

In the work reported here, we investigated DNA copy number aberrations in HCC cell lines using Affymetrix high-density SNP arrays. We identified a novel amplification at 17p11 in HCC cell lines. This region may harbor one or more genes that, when amplified, contribute to carcinogenesis. Within the amplicon, *MAPK7*, which encodes ERK5, emerged as a probable target gene that acts as a driving force for amplification of the region and promotes the growth of HCC cells by regulating entry into mitosis.

MATERIALS AND METHODS

Cell Lines and Tumor Samples

A total of 21 liver cancer cell lines [HCC-derived HLE, HLF (Dor et al., 1975), PLC/PRF/5 (Alexander et al., 1976), Li7 (Hirohashi et al., 1979), Huh7 (Nakabayashi et al., 1982), Hep3B (Aden et al., 1979), SNU354, SNU368, SNU387, SNU398, SNU423, SNU449, SNU475 (Park et al., 1995), JHH-1, JHH-2, JHH-4, JHH-5, JHH-6, JHH-7 (Fujise et al., 1990), Huh-1 (Huh et al., 1981), and the hepatoblastoma line HepG2 (Knowles et al., 1980)] were examined in this study. All cell lines were maintained in Dulbecco's modified Eagle's medium supplemented with 10% fetal bovine serum. We obtained 66 primary HCC tumors for analysis of the DNA copy number of *MAPK7* from patients undergoing surgery at the hospitals of Tokyo Medical and Dental University and Kyoto University, Japan. Genomic DNA was isolated from each cell line and from 66 primary tumors using the Puregene DNA isolation kit (Gentra, Minneapolis, MN). For immunohistochemical studies of ERK5, 43 additional HCC samples were obtained from the Hospital of Kyoto Prefectural University of Medicine, Japan. Before initiation of the present study, informed consent was obtained in the formal style approved by all relevant ethical committees.

SNP Assay

The GeneChip Mapping 100K array set and GeneChip Mapping 250K Sty array (Affymetrix, Santa Clara, CA) were used in this study. Analyses were performed according to the manufacturer's instructions. In brief, 250 ng of genomic DNA was digested with a restriction enzyme (*Xba*I or *Hind*III for the 100K array set and *Sty*I for the 250K Sty array), ligated to an adaptor, and amplified by PCR (Kennedy et al., 2003; Matsuzaki et al., 2004a,b; Zhao et al., 2004). Amplified products were fragmented, labeled by biotinylation, and hybridized to the microarrays. Hybridization was detected by incubation with a streptavidin-phycoerythrin conjugate, followed by scanning of the array, and analysis was performed as described previously (Kennedy et al., 2003; Di et al., 2005). Copy number changes were calculated using the Copy Number Analyzer for Affymetrix GeneChip Mapping Arrays (http://www.genome.umin.jp) (Nannya et al., 2005).

Fluorescence In Situ Hybridization

We performed FISH using the bacterial artificial chromosome (BAC) RP11-73E4 as a probe (Invitrogen, Carlsbad, CA) as described previously (Yasui et al., 2002). The BAC was selected

on the basis of its location according to the database provided by the UCSC (http://genome.ucsc.edu/). Briefly, the probe was labeled by nick translation with biotin-16-dUTP (Roche Diagnostics, Penzberg, Germany) and hybridized to metaphase chromosomes. Hybridization signals for biotin-labeled probes were detected with avidin-fluorescein (Roche Diagnostics).

Real-Time Quantitative PCR

We quantified genomic DNA and mRNA using a real-time fluorescence detection method. Total RNA was obtained using Trizol (Invitrogen). Residual genomic DNA was removed by incubating the RNA samples with RNase-free DNase I (Takara Bio, Shiga, Japan) prior to reverse transcription (RT)-PCR. Single-stranded complementary DNA was generated using superscript III reverse transcriptase (Invitrogen) according to the manufacturer's directions. Real-time quantitative PCR experiments were performed with the LightCycler system using FastStart DNA Master Plus SYBR Green I (Roche Diagnostics) according to the manufacturer's protocol. The primers were as follows: *MAPK7* DNA (forward, 5′-TGCTGACTGGCTCGAAG-3′; reverse, 5′-GG GTCTGAGATGAACCTGC-3′); *MAPK7* mRNA (forward, 5′-TTTGCCTTACTTCCCACCTG-3′; reverse, 5′-CCCATGTCGAAAGACTGGTT-3′); *GRAP* mRNA (forward, 5′-TCGAAGGACAGA CTGCACAC-3′; reverse, 5′-AGAAGAGGAGT GTGCCTCCA-3′); *EPN2* mRNA (forward, 5′-TCACCTCACCCACCACTGTA-3′; reverse, 5′-GTGGTCAGCTGCCCTTAGAG-3′); *EPPB9* mRNA (forward, 5′-CTTTGTGTACGGCCAG GACT-3′; reverse, 5′-CGTAGGGGTTGGTGCT TTTA-3′); *MFAP4* mRNA (forward, 5′-GGT GACTCCCTGTCCTACCA-3′; reverse, 5′-TCA TCTCAGTGCGTTTGAGG-3′); *ZNF179* mRNA (forward, 5′-ACTGGGCAGAACCAGAGAGA-3′; reverse, 5′-AGGATGCACAGACAGGCTCT-3′); *FLJ10847* mRNA (forward, 5′-AACTCTTGGG CTTCAAGCAA-3′; reverse, 5′-AGGAGGTTG AGGCTGCAGTA -3′). These primers were designed using Primer3 (http://frodo.wi.mit.edu/cgi-bin/primer3/primer3_www.cgi) on the basis of sequence data obtained from the NCBI database (http://www.ncbi.nlm.nih.gov/). *GAPDH* (Minamiya et al., 2004) and long interspersed nuclear element (LINE)-1 (Zhao et al., 2004) were used as endogenous controls for mRNA and genomic DNA levels, respectively.

Immunoblotting

Immunoblots were prepared according to previously reported methods (Yasui et al., 2001). Cell lysates (20 μg protein per sample) were separated by sodium dodecyl sulfate-polyacrylamide gel electrophoresis on 10% acrylamide gels. We obtained the following antibodies from Sigma-Aldrich (Tokyo, Japan): anti-ERK5 polyclonal antibody, anti-phospho-ERK5 (pThr218/pThr220) polyclonal antibody, and anti-β-actin monoclonal antibody. For immunoblotting, we used anti-ERK5, anti-phospho-ERK5, and anti-β-actin at dilutions of 1:500, 1:1000, and 1:5000, respectively. For secondary immunodetection, we used anti-rabbit or anti-mouse Ig (Amersham, Tokyo, Japan) diluted 1:5000. Protein binding was detected using the ECL system (Amersham).

Immunoprecipitation

Cells were lysed with RIPA buffer (10 mM Tris-HCl, pH 7.4, 150 mM NaCl, 1% Triton X-100, 0.1% sodium dodecyl sulfate, 1% sodium deoxycholate, 1 mM phenylmethylsulfonyl fluoride), and incubated on ice for 30 min. The lysate was centrifuged at 14,000 × *g* at 4°C for 15 min. The supernatant was incubated with normal rabbit IgG and protein A-agarose beads (Santa Cruz Biotechnology, Santa Cruz, CA) to decrease nonspecific protein binding. After centrifugation, the supernatant was incubated with anti-ERK5 polyclonal antibody or normal rabbit IgG (control) overnight at 4°C. Protein A-agarose beads were added to the reaction and the mixture was incubated for an additional 1 hr. The precipitates were recovered by a brief centrifugation, followed by four washes with RIPA buffer. Samples were then boiled in electrophoresis sample buffer and separated by electrophoresis as described above (see "Immunoblotting" section).

Immunohistochemical Analysis

Forty-three primary HCCs, consisting of paired tumor and surrounding nontumor tissues, and two HCC cell lines (SNU449 and Li7) were analyzed by anti-ERK5 immunostaining. Immunohistochemical staining was performed on formalin-fixed and paraffin-embedded sections using an anti-ERK5 polyclonal antibody (Sigma-Aldrich) at a 1:200 dilution. An automated tissue immunostainer (Ventana Medical Systems, Tucson, AZ) was used according to the manufacturer's instructions. The staining was developed with 3,3′-

diaminobenzidine tetrahydrochloride, followed by counterstaining with hematoxylin.

Growth Assays and RNA Interference Studies

For cell growth assays viable cells were stained with 0.2% trypan blue and counted with a hemocytometer 24, 48, and 72 hr after transfection. For RNA interference (RNAi) studies, Stealth small interfering RNA (siRNA) duplex oligoribonucleotides targeting *MAPK7* (5′-CCAUGGCAUGAAC CCUGCCGAUAUU-3′) and Stealth RNAi negative control duplexes were synthesized by Invitrogen. The siRNAs were delivered into SNU449 cells using Lipofectamine 2000 (Invitrogen) according to the manufacturer's instructions. To determine mRNA levels, cells were harvested 48 hr after transfection and subjected to quantitative RT-PCR as described above.

Cell Cycle Synchronization

SNU449 cells were synchronized at G1/S, early S, or M phases. For G1/S or early S-phase synchronization, cells were incubated in medium containing 2.5 mM thymidine (Sigma Chemical Co., St. Louis, MO) for 24 hr, followed by 12 hr in medium without thymidine, and finally another 12 hr in medium containing 2.5 mM thymidine (double-thymidine block; for G1/S-phase) or 1 μg/ml aphidicolin (early S-phase block). For M phase synchronization, cells were incubated in medium containing 2.5 mM thymidine for 24 hr, followed by 4 hr in medium without thymidine, and finally another 12 hr in medium containing 0.5 μg/ml nocodazole.

Cell Cycle Analysis

SNU449 cells were synchronized at the G1/S-phase boundary by a double-thymidine block as described above. Synchronized cells were released into fresh medium without thymidine and harvested at the indicated time points. These cells were then stained with propidium iodide and analyzed using a FACSCaliber scanner and Cell Quest software (Becton Dickinson Pharmingen, San Diego, CA).

Mitotic Index

Cells were grown in 24-well plates and transfected with Stealth RNAi targeting *MAPK7* or Stealth RNAi negative control duplexes as described above (see "Growth Assays and RNA Interference Studies" section). After 24 hr, cells were synchronized at the G1/S-phase boundary by a double-thymidine block. Synchronized cells were collected, reseeded on glass slides, and incubated for an additional 9 hr in fresh medium without thymidine. Next, the cells were stained with an anti-phospho-histone H3 antibody that specifically detects mitotic cells. Briefly, cells were fixed with 3.7% formaldehyde, permeabilized with 0.25% Triton X-100, and incubated with PBS containing 1% bovine serum albumin. The cells were then treated with a mixture of 4 μg/ml anti-phospho-histone H3 (Ser10)-biotin conjugated antibody (Upstate Biotechnology, Lake Placid, NY) and a 1:100 dilution of streptavidin-fluorescein (Roche Diagnostics) for 1 hr at room temperature, followed by counterstaining with propidium iodide. Positive staining for phospho-histone H3 was quantified by counting stained cells under a fluorescence microscope and dividing by the number of total cells. The mitotic index was scored as the percentage of mitotic cells in a population. On average, 200 cells were scored in three separate areas.

Statistical Analysis

All statistical analyses were performed using SPSS 15.0 software (SPSS Inc., Chicago, IL). Chi-square tests or analysis of variance (ANOVA) were used. P values < 0.05 were considered significant.

RESULTS

Detection of the 17p11 Amplicon in HCC Cell Lines by SNP Array Analysis

We screened for DNA copy number aberrations in 20 HCC cell lines by SNP array analysis. Two of the 20 cell lines, SNU449 and JHH-7, exhibited amplifications at chromosomal band 17p11 (Fig. 1A). In particular, the SNU449 cell line showed a high level of amplification in a narrow region on 17p11. We were able to define the smallest commonly affected region in the 17p11 amplicon as that lying between the positions recognized by the Affymetrix SNP_A-1662618 and SNP_A-1720748 probes (Fig. 1B). This region includes seven known or predicted protein-coding genes, *GRAP*, *EPN2*, *EPPB9*, *MAPK7*, *MFAP4*, *ZNF179*, and *FLJ10847*. The size of the amplicon was estimated to be approximately 750 kb.

To confirm amplification at 17p11 in SNU449 cells, we performed FISH analysis. The probe for

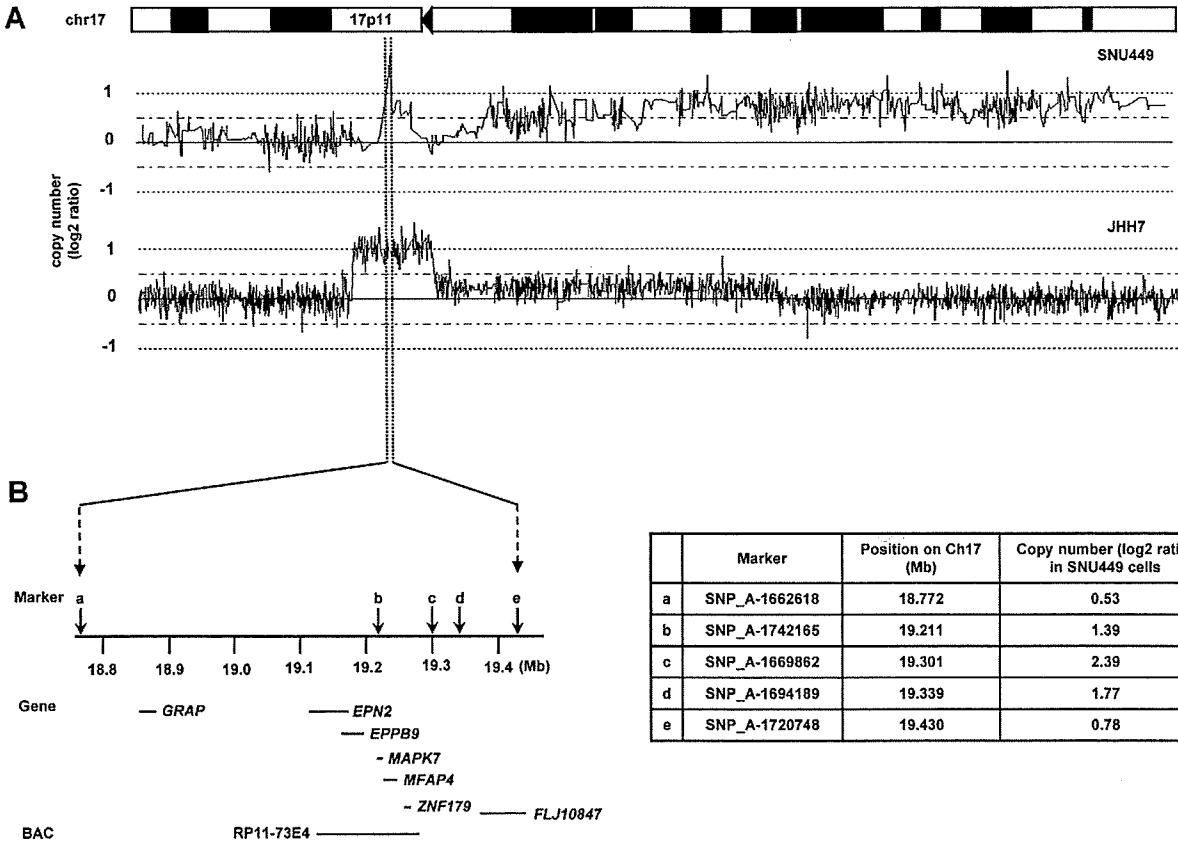

	Marker	Position on Ch17 (Mb)	Copy number (log2 ratio) in SNU449 cells
a	SNP_A-1662618	18.772	0.53
b	SNP_A-1742165	19.211	1.39
c	SNP_A-1669862	19.301	2.39
d	SNP_A-1694189	19.339	1.77
e	SNP_A-1720748	19.430	0.78

Figure 1. Map of the amplicon at 17p11 in two HCC cell lines. A: Copy number profiles for chromosome 17 in SNU449 and JHH-7 cells. Copy number values were determined by SNP 100K and 250K array analyses for SNU449 and JHH-7 cells, respectively. B: The smallest common region of amplification in SNU449 and JHH-7 cells (left). The position of the Affymetrix SNP markers, the seven genes within the amplicon (*GRAP, EPN2, EPPB9, MAPK7, MFAP4, ZNF179*, and *FLJ10847*) and the BAC RP11-73E4 (used as a probe for FISH) are numbered according to the UCSC genome database (http://genome.ucsc.edu/). Detailed copy-number information at positions identified by individual SNP markers over the amplified region in SNU449 cells is shown at right.

these experiments was BAC RP11-73E4, which contains *EPN2*, *EPPB9*, *MAPK7*, *MFAP4*, and *ZNF179* (Fig. 1B). This probe showed an amplified FISH signal on metaphase chromosomes from SNU449 cells (Fig. 2A). To further characterize the relationship between the genes in this chromosomal region and amplifications observed in cancer cells, we analyzed the gene dosage of the *MAPK7* locus by real-time quantitative PCR of DNA from 21 different liver cancer cell lines (20 HCC cell lines and the hepatoblastoma line HepG2). Amplification of *MAPK7* was observed in SNU449 and JHH-7 cells (Fig. 2B). Taken together, the data provide strong evidence that the 17p11 region is amplified in SNU449 and JHH-7 cells.

Analysis of Positional Candidate Genes in HCC Cell Lines

The 17p11 region may harbor one or more genes (henceforth referred to as "target genes") that, when activated by amplification, play a role in carcinogenesis. A common criterion for designating a gene as a putative target is that amplification leads to its overexpression (Collins et al., 1998). Thus, using real-time quantitative PCR, we determined the mRNA levels of all seven genes in the 17p11 amplicon in our panel of 21 liver cancer cell lines. As shown in Fig. 2C, the *EPN2*, *EPPB9*, and *MAPK7* genes were overexpressed in both SNU449 and JHH-7 cells. In several other lines, one or more of these three genes was overexpressed, despite the fact that regional amplification was not observed. These findings suggest that *EPN2*, *EPPB9*, and *MAPK7* are candidate target genes for 17p11 amplification.

Of these three genes, we chose to focus further analysis on *MAPK7*, which encodes ERK5, because ERK5-related proteins have been previously implicated in carcinogenesis (Hayashi and Lee, 2004; Wang and Tournier, 2006), whereas there is little or no evidence linking *EPN2* or

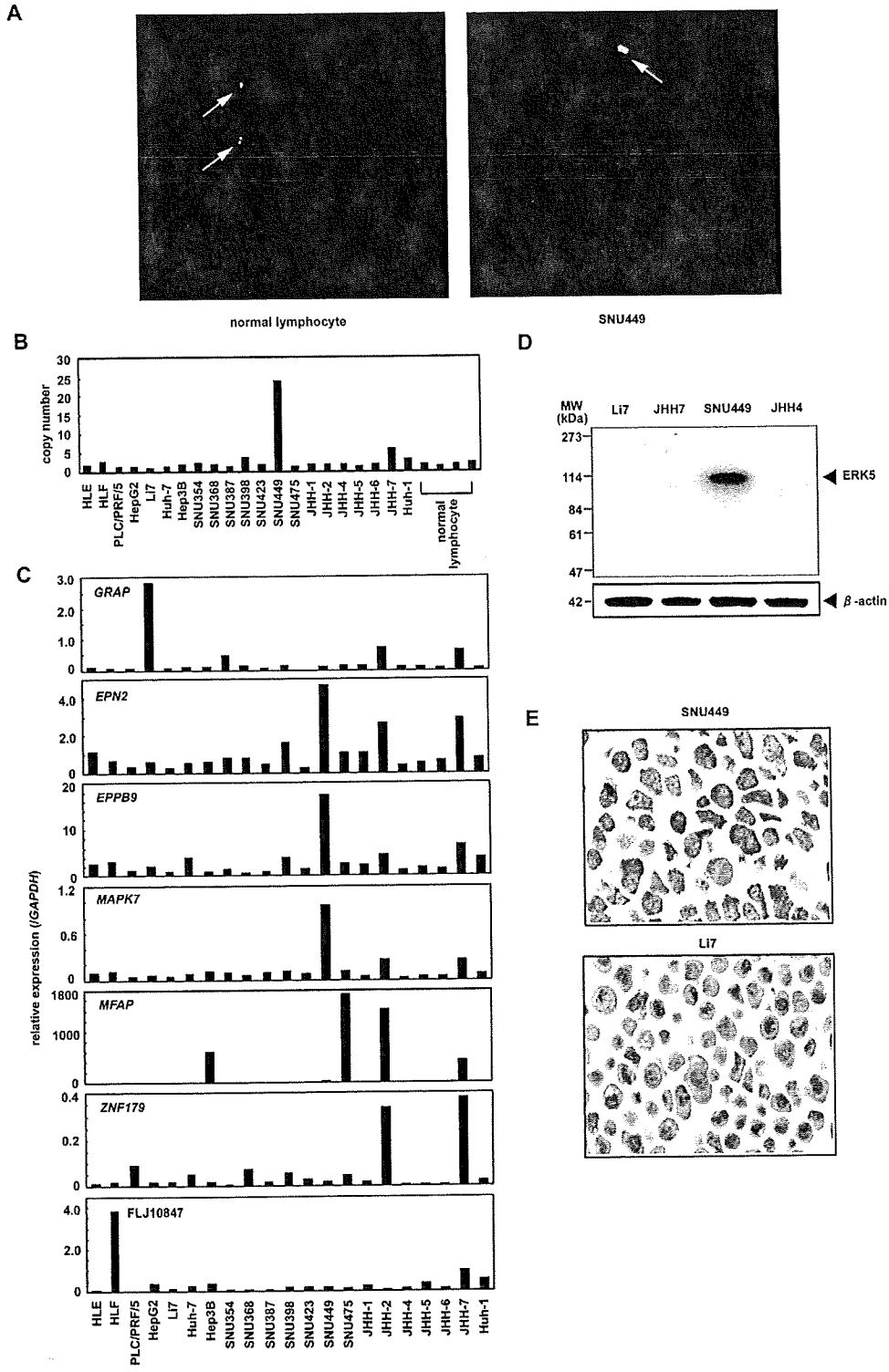

Figure 2. Amplification and overexpression of *MAPK7* in HCC cell lines. (A) Representative images from FISH analysis using a BAC RP11-73E4 probe on metaphase chromosomes from normal lymphocytes and SNU449 cells. While the probe shows a normal signal pattern (2 copies/cell) in normal lymphocytes (arrows, left), it shows an amplified signal in SNU449 cells (arrow, right). (B) Copy number of *MAPK7* in 21 liver cancer cell lines (20 HCC cells and one hepatoblastoma line, HepG2) and four peripheral blood lymphocytes (normal cell controls) as measured by real-time quantitative PCR with reference to a LINE-1 control. Values were normalized such that the average copy number of *MAPK7* in genomic DNA derived from normal lymphocytes is 2. (C) Relative expression levels of the seven genes within the 17p11 amplicon in a panel of 21 liver cancer cell lines as determined by real-time quantitative RT-PCR. The results are presented as the ratio between the expression level of each gene and a reference gene (*GAPDH*) to correct for variation in the amount of RNA. (D) Immunoblot analysis to detect protein levels of ERK5 and β-actin, an internal control, in four HCC cell lines with different *MAPK7* DNA copy numbers (B) and mRNA levels (C). (E) Immunostaining of ERK5 in SNU449 and Li7 cells.

EPPB9 to tumorigenesis. Immunoblot analysis revealed that ERK5 expression is upregulated in SNU449 cells. Indeed, among the HCC cell lines that were tested, SNU449 showed the highest level of both 17p11 amplification and *MAPK7* overexpression (Fig. 2D). Moreover, immunostaining confirmed that the level of ERK5 was elevated in SNU449 cells. ERK5 was strongly expressed in the cytoplasm of SNU449 cells (Fig. 2E). In contrast, ERK5 was weakly expressed in only a few Li7 cells, a HCC cell line that shows neither amplification nor overexpression of *MAPK7* (Fig. 2E).

Copy Number Gain of *MAPK7* in Primary HCC Tumors

To determine whether *MAPK7* is amplified in primary tumors, we examined 66 primary HCCs for copy number gains using real-time quantitative PCR. Copy number changes were counted as gains if the results of the analysis for a given tumor cell type exceeded the mean plus twice the standard deviation (SD) of the levels of *MAPK7* observed in genomic DNA derived from four peripheral blood lymphocyte samples (i.e., normal cells). A copy number gain for *MAPK7* was observed in 35 of the 66 tumors (53%; Fig. 3).

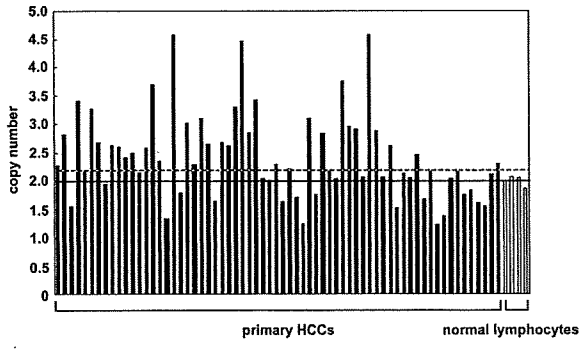

Figure 3. Copy number gain of *MAPK7* in primary HCC tumors. Copy numbers of *MAPK7* in 66 primary HCC tumors and four normal peripheral blood lymphocytes were determined by real-time quantitative PCR with reference to a LINE-1 control. Values were normalized such that the average copy number of *MAPK7* in genomic DNA derived from the normal lymphocytes equals 2 (solid horizontal line). The mean + 2 × SD of normal lymphocytes was used as the cutoff value for copy number gain (dotted line).

Expression of ERK5 in Primary HCCs

We next examined the level of ERK5 in 43 additional primary HCCs, including paired tumor and surrounding nontumor tissues. Immunohistochemical studies revealed that, in nontumor tissues (normal liver, chronic hepatitis, or liver cirrhosis), ERK5 is strongly expressed in bile ducts, bile ductules, and a few small hepatocytes (Fig. 4A). In these cells, ERK5 was present in the cytoplasm. Hepatocytes also contained ERK5, although at a lower level than in bile ducts (Fig. 4A). The staining pattern for ERK5 was almost identical for normal liver, chronic hepatitis, and liver cirrhosis.

This granular cytoplasmic staining for ERK5 was also observed in HCC cancer cells (Fig. 4B). HCC cells containing ERK5 were uniformly distributed in the tumor tissues. The level of ERK5 was elevated in 11 of the 43 tumors compared with the paired nontumor tissues (Figs. 4B and 4C; Supp. Info. Table 1). To clarify the relationship between the level of ERK5 and various clinicopathological parameters, we examined available data from the 43 patients, whose tumors were divided into elevated (T>NT) and not elevated (T≤NT) groups. There was no significant correlation between the level of ERK5 and any parameter examined, including age and gender of the patients; size, stage, and degree of differentiation of the tumor; HBV or HCV infection; and

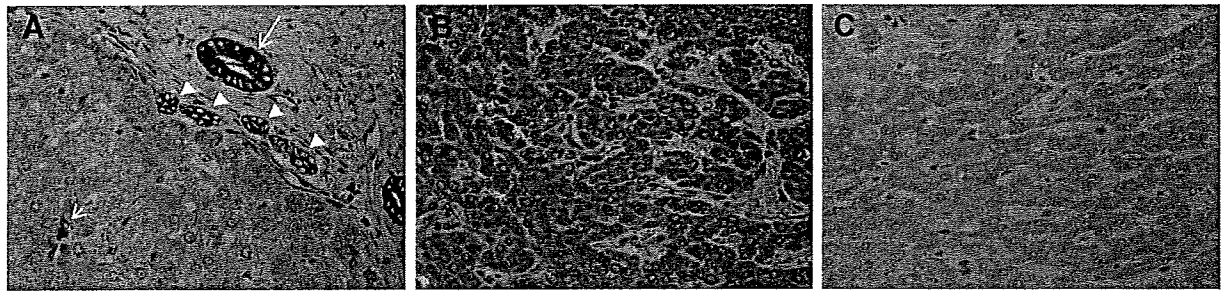

Figure 4. Representative ERK5 immunostaining of tissues. (A) A nontumorous liver tissue (chronic hepatitis). The level of ERK5 is elevated in the bile duct (large arrow), bile ductules (arrowheads), and a few small hepatocytes (small arrow). (B, C) Paired tumor (B) and nontumor (C) tissues from one HCC patient, wherein the level of ERK5 is elevated in the tumor compared with the counterpart nontumor tissue. Original magnification, ×400.

features of nontumorous liver tissues (Supp. Info. Table 1).

Downregulation of *MAPK7* Inhibits the Growth of HCC Cells

To investigate the effects of *MAPK7* overexpression on HCC cells, we knocked down its expression using RNAi. In SNU449 cells treated with siRNA targeting *MAPK7*, we observed a decrease in *MAPK7* mRNA and ERK5 protein levels relative to that observed for cells receiving a control siRNA or transfection agent alone (Figs. 5A and 5B). The siRNA-mediated downregulation of *MAPK7* suppressed the growth of SNU449 cells at all time points assayed over a 72-hr period (Fig. 5C). These findings suggest that ERK5 promotes the growth of HCC cells.

ERK5 is Phosphorylated During the G2/M Phases of the Cell Cycle

To help elucidate the underlying mechanism by which ERK5 regulates cellular proliferation we investigated the role of ERK5 in cell cycle progression. SNU449 cells were synchronized at G1/S, early S, or M phases of the cell cycle using a double-thymidine, aphidicolin, or nocodazole block, respectively. We determined the levels of total ERK5 and phosphorylated (active) form of ERK5. Immunoblotting did not show a difference in the level of total ERK5 among the three phases of the cell cycle (Fig. 6A). To detect phosphorylated ERK5, total ERK5 was immunoprecipitated from cell lysates using an anti-ERK5 antibody and then analyzed by immunoblotting using an anti-phospho-ERK5 antibody. Phosphorylated ERK5 was more abundant in cells synchronized at the M phase than in asynchronous cells (Fig. 6B).

We next synchronized SNU449 cells at the G1/S boundary using a double-thymidine block and then released the cells from the block. Using flow cytometry, we confirmed the synchrony of the cell cycle and monitored its progression after removal of thymidine (Fig. 6C). There was no difference in the level of total ERK5 during progression of the cell cycle (Fig. 6D). Expression of phosphorylated ERK was maximal 9 hr after release from the block (Fig. 6E), a time when a large proportion of cells were in the G2/M phase (Fig. 6C). Taken together, these observations indicate that ERK5 is phosphorylated during the G2/M phases of the cell cycle.

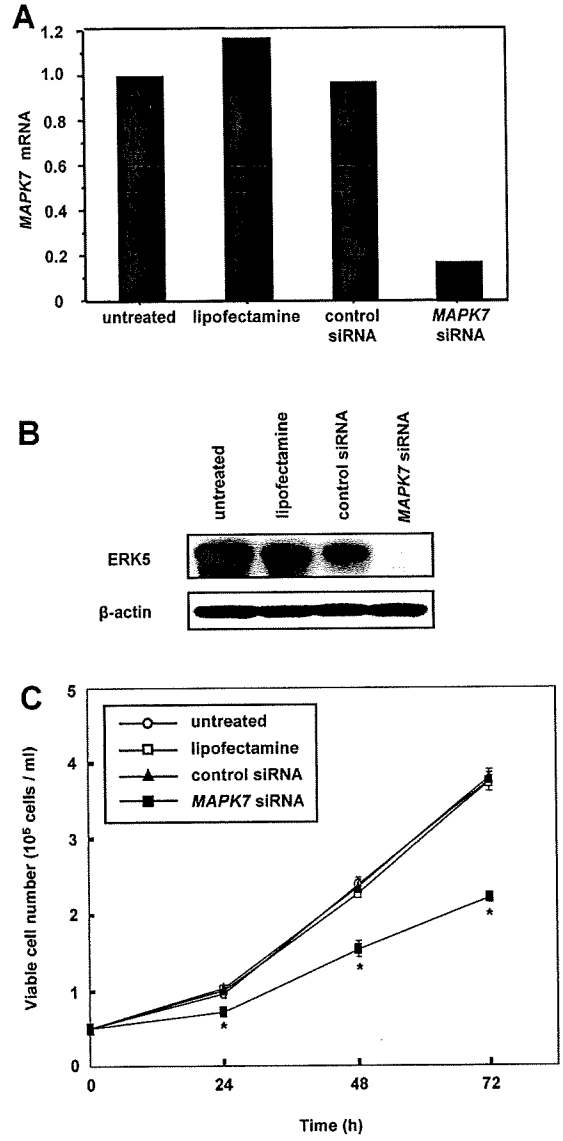

Figure 5. Growth inhibition of SNU449 cells by knockdown of *MAPK7*. A: Relative expression levels of *MAPK7* mRNA as determined by real-time quantitative RT-PCR. SNU449 cells were treated with siRNA targeting *MAPK7*, negative control siRNA, or the transfection agent alone (Lipofectamine), and harvested 48 hr after transfection. Untreated cells were maintained under identical experimental conditions. Results are presented as a ratio between the expression level of *MAPK7* and that of a reference gene (*GAPDH*) to correct for variation in the amount of RNA. Relative expression levels were normalized such that the ratio in untreated cells is 1. B: Levels of ERK5 and β-actin, an internal control, determined by immunoblotting. C: Cell growth was assayed by counting the viable cells at the indicated times after transfection. Each assay was performed in triplicate. Values are represented as the mean ± SD. Differences were analyzed by ANOVA (*$P < 0.01$).

ERK5 Regulates Entry into Mitosis

Our results indicating that ERK5 is activated during the G2/M phases in SNU449 cells suggested that ERK5 may be involved in G2/M progression. To examine whether ERK5 plays a role in mitotic entry, we knocked down *MAPK7*

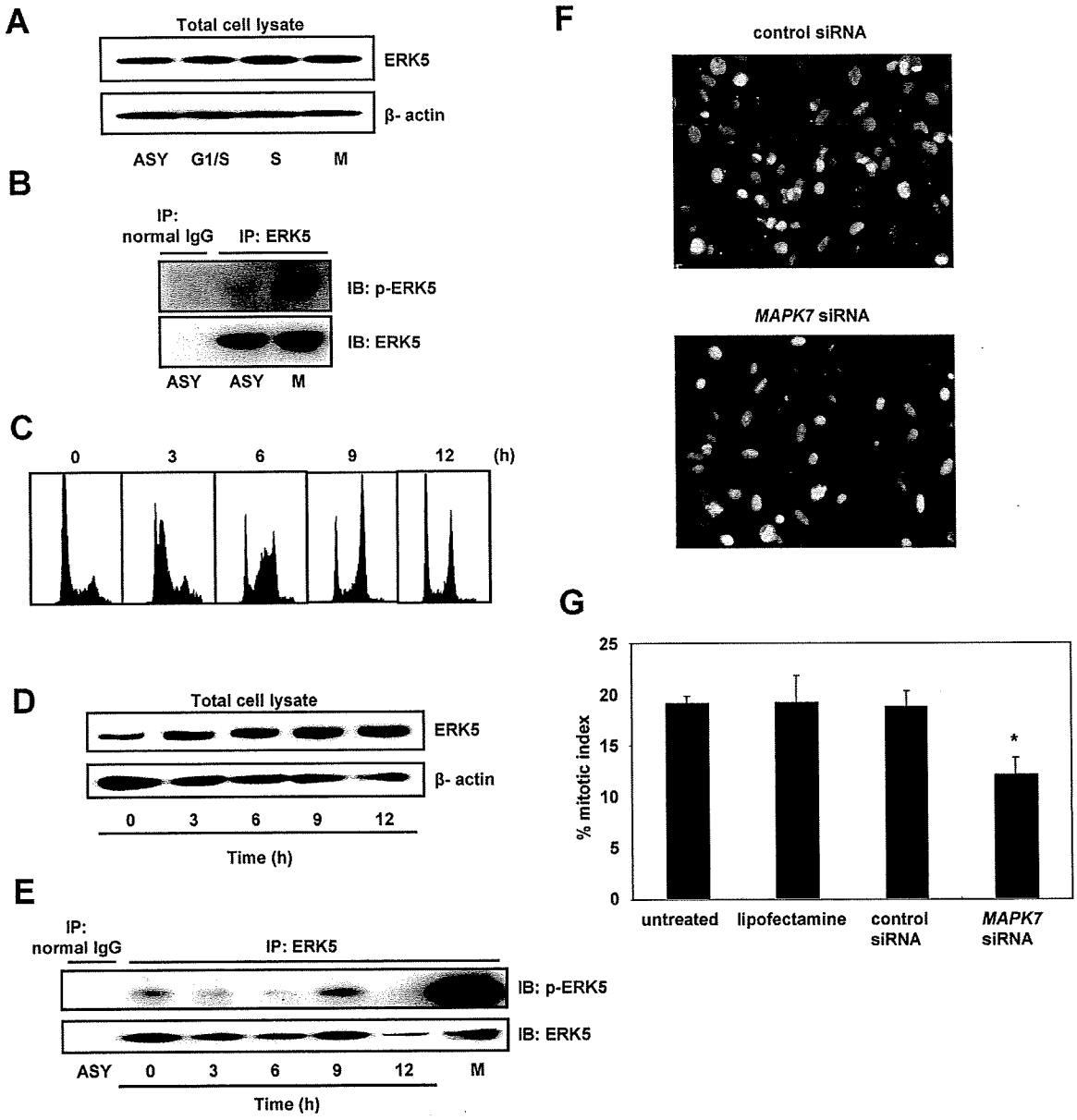

Figure 6. ERK5 is phosphorylated during the G2/M phases of the cell cycle. (A) Immunoblot analysis to detect protein levels of total ERK5 and β-actin, an internal control, in SNU449 cells that were synchronized at the G1/S, early S, or M phases using a double-thymidine, aphidicolin, or nocodazole block, respectively, or were untreated and used as an asynchronous (ASY) population. (B) Levels of phosphorylated ERK5 (p-ERK5). ERK5 was immunoprecipitated (IP) from lysates of SNU449 cells that were synchronized at the M phase (M) or from asynchronous cells (ASY). The samples were split and analyzed by immunoblotting (IB) for p-ERK5 and total ERK5. Normal rabbit immunoglobulin (normal IgG) was used as a negative control for immunoprecipitation. (C) Flow cytometric analysis. SNU449 cells were synchronized to the G1/S boundary using a double-thymidine block. Synchronized cells were released from the block and harvested at the indicated time points. The X-axis indicates DNA content and the Y-axis indicates the number of cells. (D) Time course of changes in the level of total ERK5 after release from the double-thymidine block. The level of β-actin was used as an internal control. (E) Time course of changes in the level of p-ERK5 after release from the double-thymidine block. ERK5 was immunoprecipitated from lysates of SNU449 cells harvested at the indicated times after release from the double-thymidine block. The samples were split and analyzed by immunoblotting for p-ERK5 and total ERK5. SNU449 cells, synchronized at the M phase with nocodazole, were also examined as described in (A) and (B). Normal rabbit IgG was used as a negative control for immunoprecipitation. (F) Representative images of mitotic cells in an SNU449 cell population that was transfected with *MAPK7*- or control-siRNA. SNU449 cells were treated with siRNA targeting *MAPK7*, negative control siRNA, or the transfection agent alone (Lipofectamine). Untreated cell were maintained under identical conditions. These cells were synchronized at the G1/S boundary using a double-thymidine block. The synchronized cells were released from the block and stained with anti-phospho-histone H3 9 hr after release, a time corresponding to the G2/M phase as shown in (C). Mitotic cells were identified by positive staining for phospho-histone H3 (green). Nuclear DNA was stained with propidium iodide (red). (G) The mitotic index was scored as described in Materials and Methods section. Data are presented as means ± SD (ANOVA; $^*P < 0.05$).

expression using RNAi and assessed its effect on mitosis. SNU449 cells were transfected with siRNA targeting *MAPK7* and synchronized at the G1/S-phase boundary by a double-thymidine block. The synchronized cells were released from the block and harvested 9 hr after release, a time which corresponds to the G2/M phase (Fig. 6C). Finally, harvested cells were stained with anti-phospho-histone H3 antibody, which specifically detects mitotic cells (Fig. 6F). Compared with a control siRNA or transfection agent alone, transfection of *MAPK7* siRNA significantly reduced the mitotic index (Fig. 6G). These findings suggest that ERK5 regulates mitotic entry in the HCC cells.

DISCUSSION

High-density SNP arrays are powerful tools for high-resolution analysis of DNA copy number aberrations in cancers. In the present study, using the Affymetrix GeneChip 100K and 250K SNP arrays we detected a novel amplification in HCC cells at 17p11. We were able to narrow the amplification to a 750-kb region. Notably, the amplification might have been missed using conventional analyses such as CGH. Amplification at 17p11.2-p12 has been detected in high-grade osteosarcoma using CGH (Forus et al., 1995; Tarkkanen et al., 1995). The group of van Dartel et al., (2002) established 17p11.2-p12 amplification profiles by semi-quantitative PCR using 15 microsatellite markers and seven candidate genes to assay amplification in this tumor type. They found that most of the tumors had complex amplification profiles, suggesting that multiple amplification targets, including *MAPK7*, might be present in region 17p11.2-p12. In contrast, we were able to define a smaller common region of amplification at 17p11 in two HCC cells and to determine the expression status of all genes in the amplicon. Three of the seven genes in the amplicon; *EPN2*, *EPPB9*, and *MAPK7*, were always overexpressed in cells that showed amplification in the 17p11 region. Thus, we considered these three genes as candidate targets for amplification. The function of *EPPB9* (B9 protein) is not known, and the protein encoded by *EPN2* (epsin 2) is similar to epsin 1, which plays a putative role in clathrin-mediated endocytosis (Rosenthal et al., 1999). Therefore, we focused on *MAPK7* as a target for the amplification.

Several lines of evidence implicate ERK5, which is encoded by *MAPK7*, in tumorigenesis (Wang and Tournier, 2006): (a) the ERK5 pathway is activated by Ras (English et al., 1999), ErbB (Esparis-Ogando et al., 2002; Yuste et al., 2005), Src (Sun et al., 2003), Cot (Chiariello et al., 2000), Bcr-Abl (Buschbeck et al., 2005), insulin-like growth factor-II (Linnerth et al., 2005), and interleukin-6 (Carvajal-Vergara et al., 2005); (b) ERK5 is involved in the control of breast cancer cell proliferation (Esparis-Ogando et al., 2002); (c) ERK5 mediates a survival signal that confers chemoresistance to breast cancer (Weldon et al., 2002); (d) insulin-like growth factor-II promotes cell survival via the ERK5 pathway in lung cancer cells (Linnerth et al., 2005); (e) the level of ERK5 contributes to the survival of Bcr/Abl-positive leukemic cells (Buschbeck et al., 2005); (f) ERK5 regulates cell proliferation and antiapoptotic responses in multiple myeloma (Carvajal-Vergara et al., 2005); and (g) an elevated level of MEK5, a specific activator of ERK5, is associated with metastasis and a poor prognosis in prostate cancer (Mehta et al., 2003).

The present study is the first to show the status of amplification and expression of *MAPK7* and its functional role in HCC. We found that *MAPK7* is amplified in 35 of 66 HCC tumors (53%). However, we could not determine the copy number of *MAPK7* in the nontumorous counterparts of the samples assayed because these samples were not available. Therefore, we cannot exclude the possibility that copy number polymorphism might influence the results of copy number analysis. We studied the expression of ERK5 using immunohistochemical analysis in primary HCCs and their surrounding nontumorous liver tissues. In nontumorous liver tissues, ERK5 was weakly expressed in the cytoplasm of non-neoplastic hepatocytes. Intriguingly, it was more strongly expressed in bile ducts, bile ductules, and a few small hepatocytes. In HCC tumor tissues, ERK5 was expressed in the cytoplasm of tumor cells. The level of ERK5 was elevated in 11 of 43 HCC tumors compared with their nontumorous counterparts. However, we did not observe a significant link between the level of ERK5 and any clinicopathological parameters. A recent report showed that, in prostate cancer, an increase in ERK5 cytoplasmic signals correlates with advanced disease and that strong nuclear ERK5 localization correlates with poor survival (McCracken et al., 2008).

We examined the functional roles of ERK5 in HCC cells using RNAi. Downregulation of *MAPK7* by siRNA suppressed the growth of

SNU449 cells, which had the greatest amplification and overexpression of *MAPK7* of all of the cell lines tested. These findings suggest that increased levels of ERK5 enhance the growth of HCC cells. Moreover, our results indicate that ERK5 is phosphorylated during the G2/M phases of the cell cycle and that it regulates entry into mitosis, which may explain how it promotes the growth of HCC cells.

Conflicting results have been reported by different investigators regarding the role of ERK5 in cell cycle progression. Some investigators have reported that ERK5 regulates the G1/S transition: expression of a dominant-negative form of ERK5 prevents cells from entering the S-phase of the cell cycle (Kato et al., 1998), and ERK5 can drive cyclin D1 expression (Mulloy et al., 2003). In contrast, Cude et al., (2007) and Gírio et al., (2007) recently reported that ERK5 is activated at the G2/M phases and is required for mitotic entry, findings that agree with our results.

Few molecules have been identified as direct downstream targets of ERK5. The transcriptional factors of the monocyte enhancer factor 2 family are among the best characterized substrates of ERK5. Phosphorylation of monocyte enhancer factor 2C by ERK5 enhances its transcriptional activity and subsequently leads to an increase in c-Jun gene expression (Kato et al., 1997; Wang and Tournier, 2006). A more complete identification of components downstream of ERK5 will be necessary to fully understand the role of ERK5 in carcinogenesis.

In summary, using high-density SNP arrays, we identified *MAPK7* as a probable target for the amplification events at 17p11 in HCCs. Our results suggest that the ERK5 protein product of the *MAPK7* gene plays a role in proliferation of HCC cells by regulating mitotic entry and may therefore be an optimal target for the development of novel therapies for this widespread type of cancer.

REFERENCES

Aden DP, Fogel A, Plotkin S, Damjanov I, Knowles BB. 1979. Controlled synthesis of HBsAg in a differentiated human liver carcinoma-derived cell line. Nature 282:615–616.

Alexander JJ, Bey EM, Geddes EW, Lecatsas G. 1976. Establishment of a continuously growing cell line from primary carcinoma of the liver. S Afr Med J 50:2124–2128.

Bignell GR, Huang J, Greshock J, Watt S, Butler A, West S, Grigorova M, Jones KW, Wei W, Stratton MR, Futreal PA, Weber B, Shapero MH, Wooster R. 2004. High-resolution analysis of DNA copy number using oligonucleotide microarrays. Genome Res 14:287–295.

Buschbeck M, Hofbauer S, Di Croce L, Keri G, Ullrich A. 2005. Abl-kinase-sensitive levels of ERK5 and its intrinsic basal activity contribute to leukaemia cell survival. EMBO Rep 6:63–69.

Carvajal-Vergara X, Tabera S, Montero JC, Esparís-Ogando A, López-Pérez R, Mateo G, Gutiérrez N, Parmo-Cabañas M, Teixidó J, San Miguel JF, Pandiella A. 2005. Multifunctional role of Erk5 in multiple myeloma. Blood 105:4492–4499.

Chiariello M, Marinissen MJ, Gutkind JS. 2000. Multiple mitogen-activated protein kinase signaling pathways connect the cot oncoprotein to the c-jun promoter and to cellular transformation. Mol Cell Biol 20:1747–1758.

Collins C, Rommens JM, Kowbel D, Godfrey T, Tanner M, Hwang SI, Polikoff D, Nonet G, Cochran J, Myambo K, Jay KE, Froula J, Cloutier T, Kuo WL, Yaswen P, Dairkee S, Giovanola J, Hutchinson GB, Isola J, Kallioniemi OP, Palazzolo M, Martin C, Ericsson C, Pinkel D, Albertson D, Li WB, Gray JW. 1998. Positional cloning of ZNF217 and NABC1: Genes amplified at 20q13.2 and overexpressed in breast carcinoma. Proc Natl Acad Sci USA 95:8703–8708.

Cude K, Wang Y, Choi HJ, Hsuan SL, Zhang H, Wang CY, Xia Z. 2007. Regulation of the G2-M cell cycle progression by the ERK5-NFkappaB signaling pathway. J Cell Biol 177:253–264.

Di Fiore PP, Pierce JH, Kraus MH, Segatto O, King CR, Aaronson SA. 1987. erbB-2 is a potent oncogene when overexpressed in NIH/3T3 cells. Science 237:178–182.

Di X, Matsuzaki H, Webster TA, Hubbell E, Liu G, Dong S, Bartell D, Huang J, Chiles R, Yang G, Shen MM, Kulp D, Kennedy GC, Mei R, Jones KW, Cawley S. 2005. Dynamic model based algorithms for screening and genotyping over 100 K SNPs on oligonucleotide microarrays. Bioinformatics 21:1958–1963.

Dor I, Namba M, Sato J. 1975. Establishment and some biological characteristics of human hepatoma cell lines. Gann 66:385–392.

El-Serag HB. 2002. Hepatocellular carcinoma: An epidemiologic view. J Clin Gastroenterol 35:S72–S78.

English JM, Pearson G, Hockenberry T, Shivakumar L, White MA, Cobb MH. 1999. Contribution of the ERK5/MEK5 pathway to Ras/Raf signaling and growth control. J Biol Chem 274:31588–1592.

Esparis-Ogando A, Diaz-Rodriguez E, Montero JC, Yuste L, Crespo P, Pandiella A. 2002. Erk5 participates in neuregulin signal transduction and is constitutively active in breast cancer cells overexpressing ErbB2. Mol Cell Biol 22:270–285.

Forus A, Weghuis DO, Smeets D, Fodstad O, Myklebost O, Geurts van Kessel A. 1995. Comparative genomic hybridization analysis of human sarcomas. II. Identification of novel amplicons at 6p and 17p in osteosarcomas. Genes Chromosomes Cancer 14:15–21.

Fujise K, Nagamori S, Hasumura S, Homma S, Sujino H, Matsuura T, Shimizu K, Niiya M, Kameda H, Fujita K. 1990. Integration of hepatitis B virus DNA into cells of six established human hepatocellular carcinoma cell lines. Hepatogastroenterology 37:457–460.

Garaude J, Cherni S, Kaminski S, Delepine E, Chable-Bessia C, Benkirane M, Borges J, Pandiella A, Iñiguez MA, Fresno M, Hipskind RA, Villalba M. 2006. ERK5 activates NF-kappaB in leukemic T cells and is essential for their growth in vivo. J Immunol 177:7607–7617.

Garraway LA, Widlund HR, Rubin MA, Getz G, Berger AJ, Ramaswamy S, Beroukhim R, Milner DA, Granter SR, Du J, Lee C, Wagner SN, Li C, Golub TR, Rimm DL, Meyerson ML, Fisher DE, Sellers WR. 2005. Integrative genomic analyses identify MITF as a lineage survival oncogene amplified in malignant melanoma. Nature 436:117–122.

Gírio A, Montero JC, Pandiella A, Chatterjee S. 2007. Erk5 is activated and acts as a survival factor in mitosis. Cell Signal 19:1964–1972.

Hayashi M, Lee JD. 2004. Role of the BMK1/ERK5 signaling pathway: Lessons from knockout mice. J Mol Med 82:800–808.

Hirohashi S, Shimosato Y, Kameya T, Koide T, Mukojima T, Taguchi Y, Kageyama K. 1979. Production of -fetoprotein and normal serum proteins by xenotransplanted human hepatomas in relation to their growth and morphology. Cancer Res 39: 1819–1828.

Huh N, Utakoji T. 1981. Production of HBs-antigen by two new human hepatoma cell lines and its enhancement by dexamethasone. Gann 72:178–179.

Kallioniemi A, Kallioniemi OP, Sudar D, Rutovitz D, Gray JW, Waldman F, Pinkel D. 1992. Comparative genomic hybridization for molecular cytogenetic analysis of solid tumors. Science 258:818–821.

Kato Y, Kravchenko VV, Tapping RI, Han J, Ulevitch RJ, Lee JD. 1997. BMK1/ERK5 regulates serum-induced early gene expression through transcription factor MEF2C. EMBO J 16:7054–7066.

Kato Y, Tapping RI, Huang S, Watson MH, Ulevitch RJ, Lee JD. 1998. Bmk1/Erk5 is required for cell proliferation induced by epidermal growth factor. Nature 395:713–716.

Kennedy GC, Matsuzaki H, Dong S, Liu WM, Huang J, Liu G, Su X, Cao M, Chen W, Zhang J, Liu W, Yang G, Di X, Ryder T, He Z, Surti U, Phillips MS, Boyce-Jacino MT, Fodor SP, Jones KW. 2003. Large-scale genotyping of complex DNA. Nat Biotechnol 21:1233–1237.

Knowles BB, Howe CC, Aden DP. 1980. Human hepatocellular carcinoma cell lines secrete the major plasma proteins and hepatitis B surface antigen. Science 209:97–499.

Linnerth NM, Baldwin M, Campbell C, Brown M, McGowan H, Moorehead RA. 2005. IGF-II induces CREB phosphorylation and cell survival in human lung cancer cells. Oncogene 24:7310–7319.

Little CD, Nau MM, Carney DN, Gazdar AF, Minna JD. 1983. Amplification and expression of the c-myc oncogene in human lung cancer cell lines. Nature 306:194–196.

Matsuzaki H, Dong S, Loi H, Di X, Liu G, Hubbell E, Law J, Berntsen T, Chadha M, Hui H, Yang G, Kennedy GC, Webster TA, Cawley S, Walsh PS, Jones KW, Fodor SP, Mei R. 2004a. Genotyping over 100,000 SNPs on a pair of oligonucleotide arrays. Nat Methods 1:109–111.

Matsuzaki H, Loi H, Dong S, Tsai YY, Fang J, Law J, Di X, Liu WM, Yang G, Liu G, Huang J, Kennedy GC, Ryder TB, Marcus GA, Walsh PS, Shriver MD, Puck JM, Jones KW, Mei R. 2004b. Parallel genotyping of over 10,000 SNPs using a one-primer assay on a high-density oligonucleotide array. Genome Res 14:414–425.

McCracken SR, Ramsay A, Heer R, Mathers ME, Jenkins BL, Edwards J, Robson CN, Marquez R, Cohen P, Leung HY. 2008. Aberrant expression of extracellular signal-regulated kinase 5 in human prostate cancer. Oncogene 27:2978–2988.

Mehta PB, Jenkins BL, McCarthy L, Thilak L, Robson CN, Neal DE, Leung HY. 2003. MEK5 overexpression is associated with metastatic prostate cancer, and stimulates proliferation, MMP-9 expression and invasion. Oncogene 22:1381–1389.

Mei R, Galipeau PC, Prass C, Berno A, Ghandour G, Patil N, Wolff RK, Chee MS, Reid BJ, Lockhart DJ. 2000. Genome-wide detection of allelic imbalance using human SNPs and high-density DNA arrays. Genome Res 10:1126–1137.

Minamiya Y, Matsuzaki I, Sageshima M, Saito H, Taguchi K, Nakagawa T, Ogawa J. 2004. Expression of tissue factor mRNA and invasion of blood vessels by tumor cells in non-small cell lung cancer. Surg Today 34:1–5.

Mulloy R, Salinas S, Philips A, Hipskind RA. 2003. Activation of cyclin D1 expression by the ERK5 cascade. Oncogene 22:5387–5398.

Nakabayashi H, Taketa K, Miyano K, Yamane T, Sato J. 1982. Growth of human hepatoma cells lines with differentiated functions in chemically defined medium. Cancer Res 42:3858–3863.

Nannya Y, Sanada M, Nakazaki K, Hosoya N, Wang L, Hangaishi A, Kurokawa M, Chiba S, Bailey DK, Kennedy GC, Ogawa S. 2005. A robust algorithm for copy number detection using high-density oligonucleotide single nucleotide polymorphism genotyping arrays. Cancer Res 65:6071–6079.

Nishimoto S, Nishida E. 2006. MAPK signalling: ERK5 versus ERK1/2. EMBO Rep 7:782–786.

Okamoto H, Yasui K, Zhao C, Arii S, Inazawa J. 2003. PTK2 and EIF3S3 genes may be amplification targets at 8q23-q24 and are associated with large hepatocellular carcinomas. Hepatology 38:1242–1249.

Park JG, Lee JH, Kang MS, Park KJ, Jeon YM, Lee HJ, Kwon HS, Park HS, Yeo KS, Lee KU, Kim ST, Chung JK, Hwang YJ, Lee HS, Kim CY, Lee YI, Chen TR, Hay RJ, Song SY, Kim WH, Kim CW, Kim YI. 1995. Characterization of cell lines established from human hepatocellular carcinoma. Int J Cancer 62:276–282.

Rosenthal JA, Chen H, Slepnev VI, Pellegrini L, Salcini AE, Di Fiore PP, De Camilli P. 1999. The epsins define a family of proteins that interact with components of the clathrin coat and contain a new protein module. J Biol Chem 274:33959–33965.

Sun W, Wei X, Kesavan K, Garrington TP, Fan R, Mei J, Anderson SM, Gelfand EW, Johnson GL. 2003. MEK kinase 2 and the adaptor protein Lad regulate extracellular signal-regulated kinase 5 activation by epidermal growth factor via Src. Mol Cell Biol 23:2298–2308.

Tarkkanen M, Karhu R, Kallioniemi A, Elomaa I, Kivioja AH, Nevalainen J, Böhling T, Karaharju E, Hyytinen E, Knuutila S, Kallioniemi OP. 1995. Gains and losses of DNA sequences in osteosarcomas by comparative genomic hybridization. Cancer Res 55:1334–1338.

van Dartel M, Cornelissen PW, Redeker S, Tarkkanen M, Knuutila S, Hogendoorn PC, Westerveld A, Gomes I, Bras J, Hulsebos TJ. 2002. Amplification of 17p11.2 approximately p12, including PMP22, TOP3A, and MAPK7, in high-grade osteosarcoma. Cancer Genet Cytogenet 139:91–96.

Wang X, Tournier C. 2006. Regulation of cellular functions by the ERK5 signalling pathway. Cell Signal 18:753–760.

Weldon CB, Scandurro AB, Rolfe KW, Clayton JL, Elliott S, Butler NN, Melnik LI, Alam J, McLachlan JA, Jaffe BM, Beckman BS, Burow ME. 2002. Identification of mitogen-activated protein kinase kinase as a chemoresistant pathway in MCF-7 cells by using gene expression microarray. Surgery 132:293–301.

Wong KK, Tsang YT, Shen J, Cheng RS, Chang YM, Man TK, Lau CC. 2004. Allelic imbalance analysis by high-density single-nucleotide polymorphic allele (SNP) array with whole genome amplified DNA. Nucleic Acids Res 32:e69.

Yasui K, Arii S, Zhao C, Imoto I, Ueda M, Nagai H, Emi M, Inazawa J. 2002. TFDP1, CUL4A, and CDC16 identified as targets for amplification at 13q34 in hepatocellular carcinomas. Hepatology 35:1476–1484.

Yasui K, Imoto I, Fukuda Y, Pimkhaokham A, Yang ZQ, Naruto T, Shimada Y, Nakamura Y, Inazawa J. 2001. Identification of target genes within an amplicon at 14q12-q13 in esophageal squamous cell carcinoma. Genes Chromosomes Cancer 32:112–118.

Yokoi S, Yasui K, Iizasa T, Imoto I, Fujisawa T, Inazawa J. 2003. TERC identified as a probable target within the 3q26 amplicon that is detected frequently in non-small cell lung cancers. Clin Cancer Res 9:4705–4713.

Yokoi S, Yasui K, Saito-Ohara F, Koshikawa K, Iizasa T, Fujisawa T, Terasaki T, Horii A, Takahashi T, Hirohashi S, Inazawa J. 2002. A novel target gene, SKP2, within the 5p13 amplicon that is frequently detected in small cell lung cancers. Am J Pathol 161:207–216.

Yuste L, Montero JC, Esparis-Ogando A, Pandiella A. 2005. Activation of ErbB2 by overexpression or by transmembrane neuregulin results in differential signaling and sensitivity to herceptin. Cancer Res 65:6801–6810.

Zhao X, Li C, Paez JG, Chin K, Jänne PA, Chen TH, Girard L, Minna J, Christiani D, Leo C, Gray JW, Sellers WR, Meyerson M. 2004. An integrated view of copy number and allelic alterations in the cancer genome using single nucleotide polymorphism arrays. Cancer Res 64:3060–3071.

Zhao X, Weir BA, LaFramboise T, Lin M, Beroukhim R, Garraway L, Beheshti J, Lee JC, Naoki K, Richards WG, Sugarbaker D, Chen F, Rubin MA, Jänne PA, Girard L, Minna J, Christiani D, Li C, Sellers WR, Meyerson M. 2005. Homozygous deletions and chromosome amplifications in human lung carcinomas revealed by single nucleotide polymorphism array analysis. Cancer Res 65:5561–5570.

Hepatol Int (2009) 3:403–410
DOI 10.1007/s12072-008-9108-8

CASE REPORT

Two cases of development of entecavir resistance during entecavir treatment for nucleoside-naive chronic hepatitis B

Haruhiko Kobashi · Shin-ichi Fujioka · Mitsuhiko Kawaguchi · Hiromitsu Kumada · Osamu Yokosuka · Norio Hayashi · Kazuyuki Suzuki · Takeshi Okanoue · Michio Sata · Hirohito Tsubouchi · Chifumi Sato · Kendo Kiyosawa · Kyuichi Tanikawa · Taku Seriu · Hiroki Ishikawa · Akinobu Takaki · Yoshiaki Iwasaki · Toshiya Osawa · Toshiyuki Takaki · Kosaku Sakaguchi · Yasushi Shiratori · Kazuhide Yamamoto · Daniel J. Tenney · Masao Omata

Received: 27 June 2008 / Accepted: 2 October 2008 / Published online: 9 December 2008

Abstract
Background Entecavir (ETV) is a potent nucleoside analogue against hepatitis B virus (HBV), and emergence of drug resistance is rare in nucleoside-naive patients because development of ETV resistance (ETVr) requires at least three amino acid substitutions in HBV reverse transcriptase. We observed two cases of genotypic ETVr with viral rebound and biochemical breakthrough during

H. Kobashi (✉) · A. Takaki · Y. Iwasaki · K. Sakaguchi · Y. Shiratori · K. Yamamoto
Department of Gastroenterology and Hepatology, Graduate School of Medicine, Dentistry, and Pharmaceutical Sciences, Okayama University, Okayama, Japan
e-mail: hkobashi@md.okayama-u.ac.jp

S.-i. Fujioka · M. Kawaguchi · T. Osawa · T. Takaki
Department of Medicine, Okayama Saiseikai General Hospital, Okayama, Japan

H. Kumada
Center of Liver Disease, Toranomon Hospital, Kanagawa, Japan

O. Yokosuka
Department of Medicine and Clinical Oncology, Graduate School of Medicine, Chiba University, Chiba, Japan

N. Hayashi
Department of Gastroenterology and Hepatology, Graduate School of Medicine, Osaka University, Osaka, Japan

K. Suzuki
First Department of Internal Medicine, Iwate Medical University, Morioka, Japan

T. Okanoue
Molecular Gastroenterology and Hepatology, Graduate School of Medical Science, Kyoto Prefectural University of Medicine, Kyoto, Japan

M. Sata
Department of Gastroenterology, Kurume University School of Medicine, Fukuoka, Japan

H. Tsubouchi
Digestive Disease and Life-style Related Disease Health Research, Human and Environmental Sciences, Graduate School of Medical and Dental Sciences, Kagoshima University, Kagoshima, Japan

C. Sato
Department of Analytical Health Science, Graduate School of Allied Health Sciences, Tokyo Medical and Dental University, Tokyo, Japan

K. Kiyosawa
Division of Hepatology and Gastroenterology, Department of Internal Medicine, Shinshu University School of Medicine, Matsumoto, Japan

K. Tanikawa
International Institute for Liver Research, Kurume University, Kurume, Japan

T. Seriu · H. Ishikawa
Bristol-Myers Squibb Japan, Pharmaceutical Research Institute, Tokyo, Japan

D. J. Tenney
Bristol-Myers Squibb, Research and Development, Wallingford, CT, USA

M. Omata
Department of Gastroenterology, Faculty of Medicine, University of Tokyo, Tokyo, Japan

ETV treatment of nucleoside-naive patients with chronic hepatitis B (CHB).

Results *Case 1*: A 44-year-old HBeAg-positive man received ETV 0.1 mg/day for 52 weeks and 0.5 mg/day for 96 weeks consecutively. HBV DNA was 10.0 $\log_{10}$ copies/ml at baseline, declined to a nadir of 3.1 at week 100, and rebounded to 4.5 at week 124 and 6.7 at week 148. Alanine aminotransferase (ALT) level increased to 112 IU/l at week 148. Switching to a lamivudine (LVD)/adefovir-dipivoxil combination was effective in decreasing HBV DNA. *Case 2*: A 47-year-old HBeAg-positive man received ETV 0.5 mg/day for 188 weeks. HBV DNA was 8.2 $\log_{10}$ copies/ml at baseline, declined to a nadir of 2.9 at week 124, and then rebounded to 4.7 at week 148 and 6.4 at week 160. ALT level increased to 72 IU/l at week 172. The ETVr-related substitution (S202G), along with LVD-resistance-related substitutions (L180M and M204V), was detected by sequence analysis at week 124 in both case 1 and case 2.

Conclusions ETVr emerged in two Japanese nucleoside-naive CHB patients after prolonged therapy and incomplete suppression and in one patient after <0.5 mg of dosing. ETV patients with detectable HBV DNA or breakthrough after extended therapy should be evaluated for compliance to therapy and potential emergence of resistance.

Keywords Entecavir · HBV · Chronic hepatitis B · Drug resistance · Nucleoside-naive

Introduction

Hepatitis B virus (HBV) infection is a serious health problem because of its high prevalence, estimated to be infecting more than 350 million people worldwide, and its potential for inducing chronic hepatitis, cirrhosis, hepatic decompensation, and hepatocellular carcinoma (HCC) [1, 2]. It has been demonstrated that the most potent risk factor for development of cirrhosis or HCC is serum HBV DNA level [3, 4], and it seems that suppressing serum HBV load is essential for improving the prognosis of HBV carriers. Treatment of chronic hepatitis B (CHB) has evolved markedly with the introduction of nucleoside-analogue antivirals, that is, lamivudine (LVD), adefovir-dipivoxil (ADV), entecavir (ETV), and telbivudine, to clinical practice. LVD, the first approved nucleoside analogue against HBV, was shown to be effective in suppressing HBV DNA replication, improving transaminase levels, improving liver histology, inducing hepatitis B e antigen (HBeAg) seroconversion, and suppressing hepatic insufficiency and hepatocarcinogenesis in CHB and compensated cirrhosis [5, 6]. However, the effectiveness of LVD is limited because of frequent development of drug resistance followed by a hepatitis flare and, occasionally, hepatic failure [7, 8].

ETV, a novel anti-HBV nucleoside analogue, has more than 1,500 times greater potency than LVD in vitro [9]. In clinical trials, ETV administration demonstrated potent anti-HBV activity with a marked decline in serum HBV DNA level and a significant improvement in liver histology than LVD in nucleoside-naive HBeAg-positive and -negative patients [10, 11]. In addition, emergence of ETV resistance (ETVr) or viral rebound was shown in these studies to be rare. From these results, recent treatment guidelines have recommended ETV as the first-line nucleoside analogue for nucleoside-naive CHB patients, including those with cirrhosis [12, 13].

It has been reported that the development of ETVr in nucleoside-naive patients is very rare, even after 4 years of therapy. Recently, however, rare cases of ETVr, which developed in nucleoside-naive patients in clinical studies, have been reported [14–16]. We also observed two patients who developed ETVr-associated HBV reverse transcriptase (RT) substitutions, followed by *virologic rebound*, defined as an elevation in serum HBV DNA of more than 1 $\log_{10}$ copy/ml from nadir, and biochemical breakthrough in long-term ETV treatment of nucleoside-naive CHB patients. In this article, we report these two cases in detail.

Case report

Case 1

A 44-year-old Japanese male CHB patient was positive for hepatitis B surface antigen (HBsAg), HBeAg, serum HBV DNA, and had HBV genotype C, had elevated alanine aminotransferase (ALT) levels, and had no history of nucleoside analogue treatment. The patient had a history of acute appendicitis at age 30, ureteral stone at age 35, and hyperlipidemia at age 43. He had a habit of drinking alcohol (700 ml) daily but did not smoke. At age 27, he was diagnosed for the first time by health screening as an asymptomatic HBV carrier in the immune-tolerant phase, defined by HBsAg positivity and normal liver enzymes, and he was followed up regularly elsewhere with blood tests for liver enzymes. He was found to have ALT elevation. He was referred to our hospital at age 44 and was diagnosed with CHB. Serum HBV DNA level determined by Roche Amplicor™ Monitor PCR assay (lower limit of detection is 2.6 $\log_{10}$ copies/ml = 400 copies/ml; Roche Diagnostics K.K., Tokyo, Japan) [17] was 10.0 $\log_{10}$ copies/ml and serum ALT level was 199 IU/l. Histologic diagnosis by percutaneous liver biopsy at baseline revealed chronic hepatitis with mild fibrosis and mild activity (CH F1/A1, according to the New Inuyama Classification) [18].

Table 1 Baseline characteristics

	Normal range	Unit	Case 1	Case 2
Age	–	–	44 years	47 years
Gender	–	–	Male	Male
T. Bil	0.2–1.0	mg/dl	0.8	0.5
AST	10–40	IU/l	113	48
ALT	5–40	IU/l	199	74
ALP	115–359	IU/l	268	216
BUN	6–20	mg/dl	9.5	15.9
CREA	0.61–1.04	mg/dl	0.95	0.83
ALB	4.0–5.0	g/dl	4.2	4.3
WBC	3500–8500	/μl	6,800	5,650
Hb	13.5–17.0	g/dl	15.7	14.8
PLT	13.1–36.2	10^4/μl	18.9	14.5
Prothrombin time	10–13	second	10.8	11.2
INR		–	1.0	0.9
HBsAg (CLIA)	0–0.05	IU/ml	>100 (positive)	>100 (positive)
anti-HBs (CLIA)	0–10	IU/ml	0 (negative)	0 (negative)
HBeAg (CLIA)	0–1		120 (positive)	190 (positive)
anti-HBe (CLIA)	0–50	%	<35 (negative)	0 (negative)
HBV DNA (PCR)	<2.6	$\log_{10}$ copies/ml	10.0	8.2
HBV genotype			Genotype C	Genotype C
YMDD (sequencing)			YMDD+	YMDD+
			YVDD–	YVDD–
			YIDD–	YIDD–
Liver histology[a]			CH F1/A1	CH F2/A2

[a] Diagnosed according to New Inuyama classification. T. Bil: total bilirubin, AST: aspartate aminotransferase, ALT: alanine aminotransferase, ALP: alkalinephosphatase, BUN: blood urea nitrogen, CREA: serum creatinine, ALB: serum albumin, WBC: white blood cell count, Hb: hemoglobin, PLT: platelet count, INR: international normalized ratio, HBsAg: hepatitis B surface antigen, CLIA: chemiluminescent immunoassay, anti-HBs: antibody to hepatitis B surface antigen, HBeAg: hepatitis B e antigen, anti-HBe: antibody to hepatitis B e antigen, HBV: hepatitis B virus, PCR: polymerase chain reaction, YMDD: tyrosine-methionine-aspartate-aspartate motif, YVDD: tyrosine-valine-aspartate-aspartate motif, YIDD: tyrosine-isoleucine-aspartate-aspartate motif, CH F1/A1: chronic hepatitis with mild fibrosis and mild activity, CH F2/A2: chronic hepatitis with moderate fibrosis and moderate activity

Other baseline characteristics are shown in Table 1. He was enrolled in a phase II clinical trial of ETV and was randomized into 0.1- and 0.5-mg dosage groups. The trial was conducted in Japan in compliance with the ethical principles of the Declaration of Helsinki, Good Clinical Practice guidelines, and Articles/Notifications of the Ministry of Health, Labor and Welfare (H. Kobashi et al., J Gastroenterol Hepatol, in press). He was assigned into the 0.1-mg dosage group and administered ETV at daily dose of 0.1 mg for an initial 52 weeks. Subsequently, he was administered ETV continuously at a daily dose of 0.5 mg for the following 96 weeks. The serum HBV DNA level, which was 10.0 $\log_{10}$ copies/ml at baseline, declined to a nadir of 3.1 $\log_{10}$ copies/ml at week 88 of ETV treatment. Thereafter, HBV DNA level increased from 4.5 $\log_{10}$ copies/ml at week 124 to 6.3 $\log_{10}$ copies/ml at week 140 and 6.7 $\log_{10}$ copies/ml at week 148. ALT levels increased from 28 IU/l at week 144 to 112 IU/l at week 148. The patient discontinued ETV therapy at week 148, and then received a combination therapy of 100 mg of LVD and 10 mg of ADV per day. Afterwards, HBV DNA level dropped to below 2.6 $\log_{10}$ copies/ml and ALT level was normalized after 28 weeks of LVD/ADV dosing (Fig. 1).

HBV DNA sequence analysis was performed using PCR-amplified HBV DNA from preserved serum samples at baseline and at every 24 weeks via HBV DNA polymerase sequence assay (developed at SRL, Inc., Tokyo, Japan). Although sequence analysis of the baseline isolate revealed no substitution in the RT domain of the HBV DNA polymerase gene, analysis of the isolates collected over time revealed the M204I substitution at week 100 and the L180M, S202G, and M204V substitutions at weeks 124 and 144, respectively (Table 2). In addition, a polymorphic residue N238 was found as mixed N238 N/H at week 100 and thereafter. The

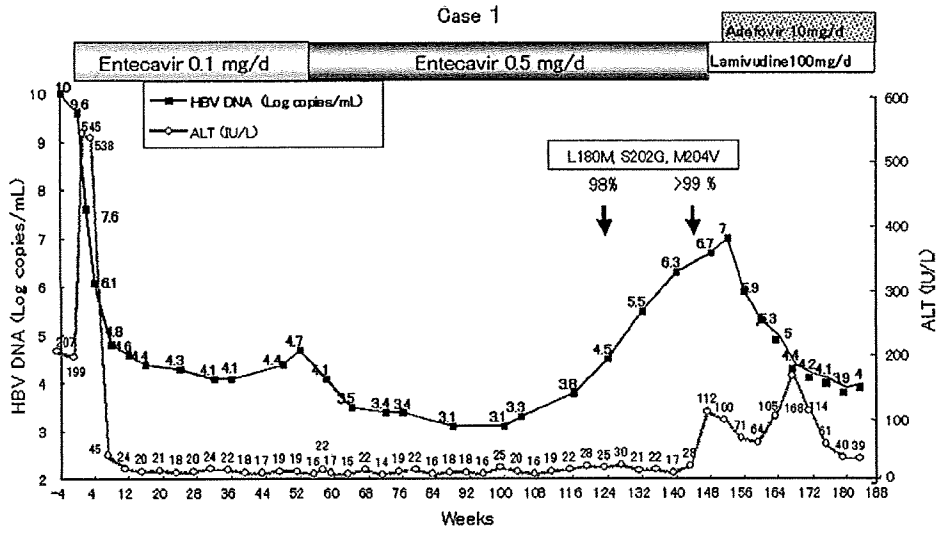

Fig. 1 Clinical course of case 1, a 44-year-old man with nucleoside-naive CHB. ETV treatment reduced ALT levels to below the upper normal limit at week 12 and reduced HBV DNA load to a nadir of 3.1 $\log_{10}$ copies/ml at week 88. However, HBV DNA re-elevated to 4.5 $\log_{10}$ copies/ml at week 124 (virologic breakthrough) and 6.3 $\log_{10}$ copies/ml at week 140, as well as ALT level re-elevated at week 148 (biochemical breakthrough). Sequence analysis of the HBV DNA polymerase gene using serum sample obtained at weeks 124 and 144 revealed the emergence of L180M, M204V (related to LVD resistance), and S202G (related to ETVr) substitutions. SNP-PCR assay revealed that LVDr M204V and ETVr S202G substitutions were detected first at week 124 (98%) and increased at week 148 (>99%). Switching from ETV to LVD/ADV combination treatment at week 148 was successful in reducing HBV DNA load and ALT again

Table 2 Population sequence analysis of isolates from case 1 on ETV therapy

Week	Reverse transcriptase position				
	180	202	204	223	238
0	L	S	M	S/A	N
24	L	S	M	S/A	N
100	L	S	M/I	S/A	N/H
124	M	G	V	S	N/H
144	M	G	V	S	N/H

polymorphic residue S223, which was mixed as S/A at baseline, was found to be only S at weeks 124 and 144.

In addition, preserved serum samples from this patient at baseline and at every 24 weeks were analyzed by an ultrasensitive, single-nucleotide-polymorphism (SNP)-PCR assay, using a method similar to Punia et al. [19] for identification of resistance substitutions, as well as analyzing the sequence of individual clones to determine the genetic linkage of substitutions. SNP-PCR analysis was performed for the two LVD-resistance (LVDr) substitutions, M204V (codon GTG) and M204I (codons ATA and ATT), and the ETVr substitution S202G. Both wild-type and positive control plasmids containing the correct sequence were used at various concentrations to establish the background level as well as the level of detection for each substitution. For clonal analysis, the amplified RT gene from the patient's HBV was cloned into plasmids, as well as 22 to 24 individual clones were selected and sequenced, to determine the genetic linkage of the different substitutions observed.

SNP-PCR analysis for ultrasensitive detection of the resistance substitutions revealed that the LVDr M204V(GTG) and ETVr S202G(GGT) substitutions were not detected (<0.1%) at baseline, week 24, or week 100. The M204I substitution (codon ATA) was detected at low levels at week 24 (0.4%), increased levels at week 100 (6.6%), and was present but at reduced levels at weeks 124 and 148 (0.4% at both time points). The LVDr M204V and ETVr S202G substitutions were detected first at week 124 (98%) and increased levels at week 148 (>99%). The levels of M204I(ATA) were lower at weeks 124 and 144, likely as a result of the dominant M204V/S202G virus (Table 3). Samples at weeks 48 and 76 could not be analyzed conclusively because of low yields of HBV DNA from serum samples.

Clonal analysis revealed that position 223 was a mixture of S and A residues at baseline, the LVDr substitutions L180M and M204V, as well as the ETVr substitution S202G, all emerged simultaneously and were linked in the same virus isolate clones at week 124, isolates that also contained S at position 223. These substitutions did not appear to arise from the LVDr isolates with M204I because the M204I substitution emerged in an isolate with substitution S223A.

Table 3 SNP-PCR analysis of case 1 isolates

Week	M204V		S202G		M204I (ATA)		M204I (ATT)	
	Mut/WT	Ave (%)	Mut/WT	Ave (%)	Mut/WT	Ave (%)	Mut/WT	Ave (%)
0	1/5,424	0.018	1/15,453	0.0065	1/4,199	0.024	1/37,940	0.0026
24	1/5,655	0.018	1/19,000	0.0052	**1/243**	**0.410**	1/46,518	0.0021
100	1/3,846	0.026	1/16,038	0.0062	**1/14**	**6.569**	1/50,456	0.0020
124	**48/1**	**97.973**	**59/1**	**98.327**	**1/265**	**0.377**	1/12,879	0.0078
144	**706/1**	**99.859**	**1,250/1**	**99.920**	**1/237**	**0.421**	1/10,573	0.0095

Cells with bold and underlined font are considered positive (>1/1000 or >0.1% mutant/wild-type)

Mut/WT, mutant/wild type, mean ($N = 3$)

Ave %, average % in total HBV DNA

Case 2

A 47-year-old Japanese male CHB patient was positive for HBsAg, HBeAg, serum HBV DNA, and had HBV genotype C, had elevated ALT levels, and had no history of nucleoside analogue treatment. At age 33, he was diagnosed for the first time as an asymptomatic HBV carrier in the immune-tolerant phase because of positive HBsAg and normal liver enzymes. At age 44, he was found to have ALT elevation, referred to our hospital, and diagnosed with CHB. Histologic diagnosis by percutaneous liver biopsy revealed chronic hepatitis with moderate fibrosis and moderate activity (CH F2/A2 according to the New Inuyama Classification). He was treated with ursodeoxycholic acid at a daily dose of 600 mg orally and glycyrrhizin preparation (stronger Neo-Minophagen C™) 40 ml i.v. thrice per week for 3 months. However, liver enzymes did not normalize. Interferon-α2b administration, three mega units i.m. thrice per week, was started at age 45 and continued for 24 weeks. Although HBV DNA level was reduced transiently to below 3.7 $\log_{10}$ copies/ml at the end of therapy, it rose 9 months after cessation of interferon therapy to 8.2 $\log_{10}$ copies/ml and ALT level increased to 483 IU/l. At age 47, the patient was started on ETV treatment as the subject enrolled in the ETV clinical trial (ETV-053) in Japan at a daily oral dose of 0.5 mg and continued for 188 weeks. A liver biopsy performed 1 month before starting the ETV treatment showed chronic hepatitis with moderate fibrosis and moderate activity (CH F2/A2, according to the New Inuyama Classification). The baseline serum HBV DNA level was 8.2 $\log_{10}$ copies/ml, ALT level was 74 IU/l, and other baseline characteristics were as shown in Table 1. The serum HBV DNA level declined to 3.2 $\log_{10}$ copies/ml and ALT level decreased to below the upper limit of normal at week 32. Liver histology improved to mild-to-moderate fibrosis and mild activity (CH F1-2/A1) at week 48 and chronic hepatitis with mild-to-moderate fibrosis and mild activity (CH F1/A1) at week 148. HBV DNA level was suppressed to a nadir of 2.9 $\log_{10}$ (794) copies/ml at week 124 and rose again to 4.7 $\log_{10}$ copies/ml at week 148, 5.4 $\log_{10}$ copies/ml at week 152, and 6.4 $\log_{10}$ copies/ml at week 160 and 7.0 $\log_{10}$ copies/ml at week 164. ALT level rose to 79 IU/l at week 172 and remained between 40 and 50 IU/l thereafter. ETV at 0.5 mg/day was continued until this time (Fig. 2).

HBV DNA sequence analysis revealed no resistance substitutions in the patient's baseline virus. However, the LVDr-related substitutions L180M and M204V, as well as ETVr-related substitution S202G, were detected at week 124, as a mixed population with wild type, and at week 148, as a pure population (Table 4). In addition, the patient displayed evidence of several polymorphic substitutions at baseline, indicating a mixed quasi-species, which became enriched for those with the resistant virus over time.

SNP-PCR analysis was used to determine the first appearance of the resistance substitutions, using the same method as for case 1. There was no antiviral resistance detected at baseline (<0.1%). The M204V (0.65%) and S202G substitutions were detected first at week 24 but not again until week 124. At weeks 124 and 148, the resistant isolate had become enriched to 43% (M204V) and 98% (M204V), respectively (Table 5).

Clonal analysis was performed to determine the genetic linkage of the various substitutions observed, using the same method as for case 1. The amplified RT gene from the patient's virus was cloned into plasmids, and 24 to 27 individual clones were selected and sequenced. From the clonal analysis, it can be seen that there are three positions that contain mixtures at baseline; position 55 is a mixture of H and R residues, position 221 is a mixture of Y and F residues, and position 269 is a mixture of I and L residues. The substitutions L180M and M204V, as well as the ETVr-related substitution S202G, all emerge simultaneously and in an isolate with H at position 55, Y at position 221, and I at position 269.

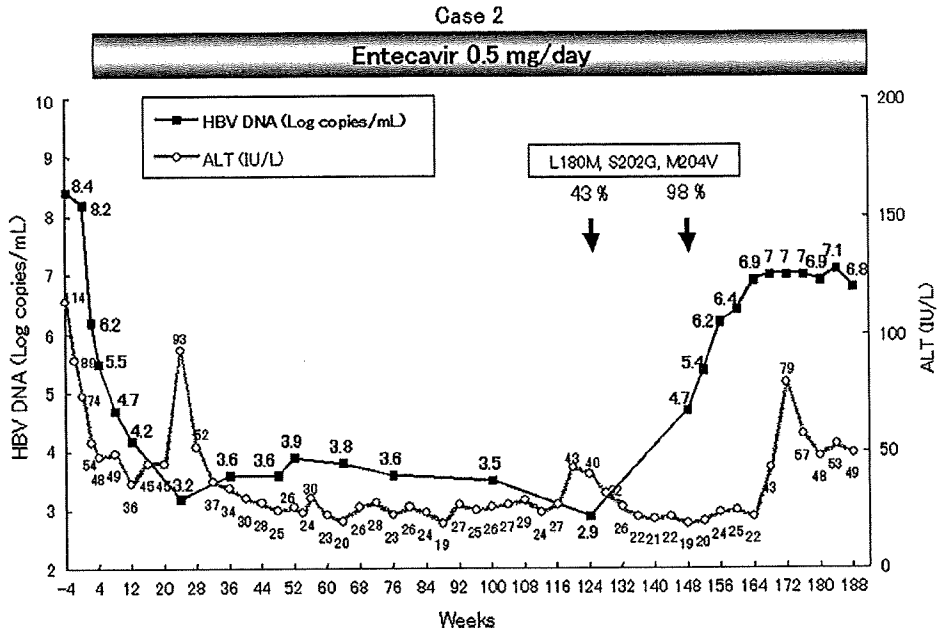

Fig. 2 Clinical course of case 2, a 47-year-old man with nucleoside-naive CHB. ETV treatment reduced ALT level to below the upper normal limit at week 30 and reduced serum HBV DNA level to a nadir of 2.9 $\log_{10}$ copies/ml at week 124. However, HBV DNA level re-elevated to 4.7 $\log_{10}$ copies/ml (virologic breakthrough) at week 148 and 7.0 $\log_{10}$ copies/ml at week 168, as well as ALT level re-elevated to 79 IU/l at week 172. Sequence analysis of the HBV DNA polymerase gene using serum sample obtained at weeks 124 and 148 revealed the emergence of L180M, M204V (related to LVD resistance), and S202G (related to ETVr) substitutions. SNP-PCR assay revealed that the resistant isolate was enriched to 43 (M204V) and 98% (M204V), respectively

Table 4 Population sequence analysis of isolates from case 2 on ETV therapy

Week	RT position								
	55	76	180	191	195	202	204	221	269
0	H/R	S	L	V	F	S	M	Y/F	I/L
24	H/R	S	L	V	F	S	M	Y/F	I/L
52	H/R	S	L	V	F	S	M	Y/F	I/L
100	H	S	L	V	F	S	M	Y/F	I/L
124	H	S/T	L/M	V/I	F/S	S/G	M/V	Y	I/L
148	H	S	M	V	F	G	V	Y	I

Table 5 SNP-PCR analysis of case 2 isolates

Week	S202G[a]	M204V (GTG, %)	M204I (ATA, %)	M204I (ATT, %)
0	Negative	0.016	0.020	0.0065
24	Positive	0.65	0.029	0.018
52	Negative	0.021	0.020	0.018
100	Negative	0.020	0.021	0.010
124	Positive	43	0.33	0.010
148	Positive	98	2.9	0.016

[a] S202G PCR was non-quantitative. A positive indicates 4-fold, 5085-fold, and 10475-fold the wild-type background for weeks 24, 124, and 148, respectively. The baseline isolate gave 1.1-fold the wild-type background

Discussion

The most important limitation of long-term nucleoside analogue treatment for CHB is the emergence of drug-resistant mutant HBV followed by viral breakthrough and hepatitis flare [12]. The most common mutation associated with LVDr involves substitution of methionine in the tyrosine-methionine-aspartate-aspartate (YMDD) motif of the HBV DNA polymerase gene RT domain with valine or isoleucine (M204V/I), with or without a leucine-to-methionine substitution in an upstream region (rtL180M) [20]. It was reported that LVDr was detected at a rate of 14 to 32% after 1 year and 60 to 70% after 5 years of LVD treatment [12]. The substitutions conferring resistance to ADV are asparagine to threonine (N236T) and alanine to valine or threonine (A181V/T) [21], and the cumulative probability of ADV resistance with elevation of HBV DNA level has been reported to be 20% at 5 years in HBeAg-negative patients [22] and as high as 42% in HBeAg-positive patients [23].

In the case of ETV, it has been reported that resistance to the drug requires at least one of three substitutions in HBV RT, that is, rtT184, rtS202, and rtM250, as well as LVDr-related substitutions rtL180M and M204V [24]. Phenotypic analyses of samples associated with virologic breakthrough confirmed that ETV susceptibility correlates